A MECHANISTIC VIEW ON rRNA – ANTIBIOTICS BINDING

by

Mehmet Ünal Güneş

B.S., Genetics and Bioengineering, Yeditepe University, 2009

Submitted to the Institute for Graduate Studies in
Science and Engineering in partial fulfillment of
the requirements for the degree of
Master of Science

Graduate Program in Chemical Engineering

Boğaziçi University

2011

ACKNOWLEGMENTS

First of all, I would like to express my truthful gratitude to my thesis supervisor Prof. Türkan Haliloğlu, who devoted his valuable time to guiding me, helping me and motivating me all the time. I am so happy to study under her supervision in Polymer Research Center. I also thank to Assoc. Prof. Işıl Aksan Kurnaz and Prof. Pemra Doruker Turgut, who has read and commented on my thesis.

Special thanks to Azize Yıldız, Perihan Ünver, Kadir Özden, Orhan Özden, Çağlar Meriçer, Duygu Kocaman, Şefik Kerem Ovalı, Arzu Uyar, Fidan Sümbül, Cihan Kaya, Merve Eropak and Bahar Nalbantoğlu, who devoted their valuable time to help and motivate me all the time. I also wish to express my gratitude to all members of Polymer Research Center for their suggestions and friendships.

Heartfelt thanks to my comrades, İhsan Ömür Akdağ, Mehmet Tarık Can, Melek Selcen Başar, Aslıgül Doğan, Gülsüm Ersoy, Aybüke Leba, İpek Paksoy, Caner Ülgüel, Simay Yalaz, Burcu Yoğurtçu, Okan Yüzüak, Dilek Eren, Özer Özcan, Mehmet İrfan Hösükoğlu, Nilay Aktürk, Sıla Kumbasar, Murat Erol, Ahmet Özcan, Ali Uzun for giving me their everlasting friendship and joyful help all the time.

Finally, I would like to thank my family for their unrequited support and trust in me throughout my thesis like my whole life. This work is dedicated to them, without whom it would have never been possible.

ABSTRACT

A MECHANISTIC VIEW ON rRNA – ANTIBIOTICS BINDING

The ribosome, which is the macromolecular machine for protein synthesis, is one of the most striking targets for the antimicrobial drugs. Antibiotics that block the protein synthesis in various ways in ribosome have different modes of action and binding sites in different microorganisms. The key interactions are mainly between ribosomal RNA (rRNA) and antibiotics. The interaction sites of these antibiotics with the rRNA, determined by biochemical, *in vitro* and *in vivo* cross-linking experiments and footprinting studies, are proved when the structures with antibiotics are discovered. We used the Gaussian Network Model (GNM) to predict antibiotic binding sites and their interactions with the ribosomal proteins. In the GNM, the structures are modeled as an elastic network, where the inter-residue interactions are harmonic. We have analyzed the vibrational modes of motion for 73 ribosome structures (64 bound, 9 unbound) from *Deinococcus radiodurans, Escherichia coli, Haloarcula marismortui* and *Thermus thermophilus*. We propose a mechanistic view for the antibiotics binding and to predict antibiotic binding sites and their interactions with the ribosomal proteins based on the dynamics of rRNA. The antibiotics binding sites are mainly located at the Peptidyl Transferase Center (PTC) and decoding center in 23S rRNA and 16S rRNA, respectively. The nucleotides showing high frequency fluctuations cluster in two regions and these two regions correspond to these two functional and known antibiotics binding sites. The nucleotides in the antibiotics binding sites and their adjacent nucleotides form a network of residues that are coupled in their high frequency fluctuations. This network may also lead to the allosteric interaction between the antibiotics binding sites and ribosomal proteins.

ÖZET

rRNA - ANTİBİYOTİK BAĞLANMARI ÜZERİNE MEKANİSTİK BİR BAKIŞ

Protein sentezi için makromoleküler bir makina olan ribozom antimikrobiyal ilaçlar için çok önemli bir hedefdir. Protein sentezini ribozomda değişik yollarla engelleyen antibiyotikler değişik mikroorganizmalarda değişik aksiyon modları, bağlanma bölgeleri ve konformasyonlara sahiptir. En önemli etkileşmeler genellikle ribozomal RNA (rRNA) ve antibiyotikler arasındadır. Biyokimyasal, *in vitro* ve *in vivo* çapraz bağlantılı deneyler ve footprinting çalışmaları ile belirlenen rRNA ile antibiyotikler arasındaki etkileşme bölgeleri antibiyotikleri içeren yapıların bulunmasıyla kanıtlandı. Bu tez çalışmasında antibiyotik bağlanma bölgelerini ve onların ribozomal proteinler ile olan etkileşmelerini bulmak için Gaussian Ağyapı Modelini (GNM) kullandık. Gaussian Ağyapı Modelininde RNA yapılar rezidüler arasındaki etkileşimlerin harmonik olduğu bir elastik ağyapı olarak modellenir. *Deinococcus radiodurans, Escherichia coli, Haloarcula marismortui* ve *Thermus thermophilus* canlılarından 73 ribozom yapısının (64 antibiotik bağlı, 9 antibiyotik bağlı olmayan) hareketinin titreşimsel modlarını inceledik. Antibiyotik bağlanması ve onların bağlanma bölgeleri ve ribozomal proteinler ile etkileşmelerini hesapsal olarak tahmin edebilmek için rRNA dinamiğine bağlı mekanistik bir perspektif sunuyoruz. Antibiyotik bağlanma bölgeleri genellikle büyük ribozomal altbiriminde Peptidil Transfer Merkezine ve küçük ribozomal altbiriminde kodonun okunduğu bölgelerdir. Yüksek frekansta dalgalanma gösteren nükleotidler iki bölgede toplanıyor ve bu bölgeler fonksiyonel ve bilinen antibiyotik bağlanma bölgelerine denk geliyor. Bağlanma bölgelerinde bulunan yüksek frekans dalgalanmalarındaki nükleotidler ve bu nükleotidlerin komşusu olan nükleotidler bir ağyapı oluşturuyor. Bu network ayrıca antibiyotik bağlanma bölgeleri ve ribozomal proteinler arasındaki allosterik etkileşimede de rol oynayabilir.

TABLE OF CONTENTS

LIST OF FIGURES

LIST OF TABLES

LIST OF SYMBOLS

r_c	Cutoff distance
$\mathbf{R}_i$	Instantaneous position vector of residue *i*
$\mathbf{R}_i^o$	Equilibrium position vector of residue *i*
u	Eigenvector of the connectivity matrix
V_{GNM}	Potential of GNM
Å	Angstrom
λ	Eigenvalue of the connectivity matrix
γ	Force constant
Γ_{ij}	Kirchhoff matrix element of residues *i* and *j*
$\Delta\mathbf{R}_i$	Fluctuation vector of residue *i*
$\langle\Delta\mathbf{R}_{ij}^2\rangle$	Relative mean square fluctuation of residue *i* and *j*

LIST OF ACRONYMS/ABBREVIATIONS

A site	Aminoacyl site
ACC	Accuracy
D.r.	Deinococcus radiodurans
E site	Exit site
E. c.	Escherichia coli
EFs	Elengoation Factors
FN	False Negatives
FP	False Positives
GNM	Gaussian Network Model
H.m.	Haloarcula marismortui
IFs	Initiation Factors
mRNA	Messenger RNA
P site	Peptidyl site
PDB	Protein Data Bank
PRE	Precision
PTC	Peptidyl Transferase Center
RFs	Release Factors
rRNA	Ribosomal RNA
SN	Sensitivity
SP	Specificity
TN	True Negatives
TP	True Positives
tRNA	Transfer RNA
T.t.	Thermus thermophilus

1. INTRODUCTION

Ribosomes are the ribonucleoproteins which translate the genetic code provided by mRNA into the proteins in the translation mechanism. In prokaryotes, ribosome is composed of two subunits. The large subunit (50S) is composed of 23S rRNA which comprises approximately 2900 nucleotides, 5S rRNA (approximately 120 nucleotides) and approximately 30 proteins. The peptide bond synthesis occurs in the Peptidyl Transferase Center (PTC) which is the most common antibiotic binding site in this subunit. Other binding sites in this subunit include exit (E) site, aminoacyl (A) site, peptidyl (P) site and the entrance of exit tunnel of nascent polypeptide chains. The small subunit (30S) is composed of 1500 nucleotides long 16S rRNA and about 20 proteins. The decoding of mRNA is carried out in 30S subunit with appropriate tRNA binding to A, P and E sites. Although ribosomal proteins take role in weak interactions in some antibiotic bound cases, rRNA is the major target of the antibiotics [1].

The 23S rRNA binding antibiotics such as macrolides [1-7], ketolides [2, 6, 8, 9], lincosamides and phenicols like chloramphenicol [1, 6] have different ways to prevent protein synthesis. One of the ways is to bind to the A site as in the case oxazolidinone linezoid [10] and affecting the tRNA positioning and as a result blocking the peptide bond synthesis. Antibiotics like erythromycin, clarithromycin, and roxithromycin, which belong to the 14-member-ring macrolide class, sterically block the nascent polypeptide chain exit tunnel instead of directly blocking the PTC. Macrolides blocking exit tunnel reduce the diameter of the tunnel from 18-19 Å to less than 10 Å [1]. Troleandomycin, a semi-synthetic macrolide, also blocks the tunnel and rearranges the tunnel wall conformation by changing the conformation of ribosomal protein L22 [3]. Ketolides, derivatives of macrolides, do not have cladinose sugar compared to macrolides which have lactone ring, desosamine sugar and cladinose sugar, and they bind tighter to ribosomes than macrolides [1]. Telithromycin, as a ketolides, functions by blocking the exit tunnel of nascent polypeptide chains [8].

Ribosomal proteins have less effect on antibiotics binding, but sometimes they involve in antibiotics resistance such as in macrolides like erythromycin. Mutations on L4 (R111 D.r./K90 E.c.) and L22 (G63 D.r./G64 E.c.) proteins may perturb the rRNA structure and that generates erythromycin resistance although they are not in a close distance close with the antibiotics to form strong chemical interactions [1, 11]. L22 has a gating role of ribosome exit tunnel. L32 also forms interactions with troleandomycin in *Deinococcus radiodurans* [3]. Mutations of L3 on the R144 and K145 D.r. have a remote effect on antibiotics binding when it is supported by the mutation in 23S rRNA [12].

Some nucleic acids are highly important in antibiotics binding in both different antibiotics binding to ribosome and antibiotics binding to different microorganisms. Sparsomycin and streptogramins [13], bind to A2602 (*E. coli* numbering system is used throughout the text unless otherwise stated), which is a highly flexible nucleotide in PTC, and alters the A, P sites and PTC conformation [14]. U2584 is important in A-site antibiotics binding and A2058 has substantial effect on binding of macrolides, lincosamides and streptogramins B (MLS_B) [8, 12]. A2585 is important for positioning of P-site substrates by affecting the positioning of 3' end of P-site bound tRNA [13] and for tiamulin binding [12].

Upon the advancements on the crystal structure determination of ribosome complexed with antibiotics, the binding sites of antibiotics and their mode of action has become more obvious. However, to determine every complex ribosome structure is not an easy issue since it is a huge macromolecule and there are various potential drugs that has to be validated. Here we investigated the antibiotics binding on 73 ribosome structures (64 bound, 9 free) from 4 different microorganisms; *Deinococcus radiodurans*, *Escherichia coli*, *Haloarcula marismortui* and *Thermus thermophilus*. Our study is based on the prediction of interaction sites via GNM, which is a coarse grained elastic network model, and determination of allosteric interactions of antibiotics with ribosomal proteins.

2. RIBOSOMES AND ANTIBIOTICS

2.1. Ribosomes and Translation

Translation of RNA to protein occurs in ribosomes. Synthesis of proteins needs a very complex mechanism including mRNA, tRNA, rRNA, initiation factors (IFs), elongation factors (EFs) and release factors (RFs) that take role in ribosome recycling. In recycling mechanism the two subunits of ribosome constitute a complex ribosome structure and then they dissociate. The bacterial 70S ribosome is formed by large (50S) and small (30S) subunit [15]. The genetic code is transferred from DNA to RNA in transcription mechanism. The complementary copies of genes are transcribed to the mRNA molecules. These mRNA molecules binds to ribosomes, sandwiched between the large and small ribosomal subunits and translation mechanism occurs by the help of tRNA which helps to bring the suitable amino acid, which is coded in the mRNA sequence, to the ribosome [16].

The translation mechanism is shown in the Figure 2.1. Ribosome consists of aminoacyl (A), peptidyl (P), and exit (E) sites where codon sequence of mRNA and anticodon sequence of tRNA match. During elongation of the nascent chain polypeptide, tRNA bound to the amino acid coded by codon enters the A site and peptide bond occurs

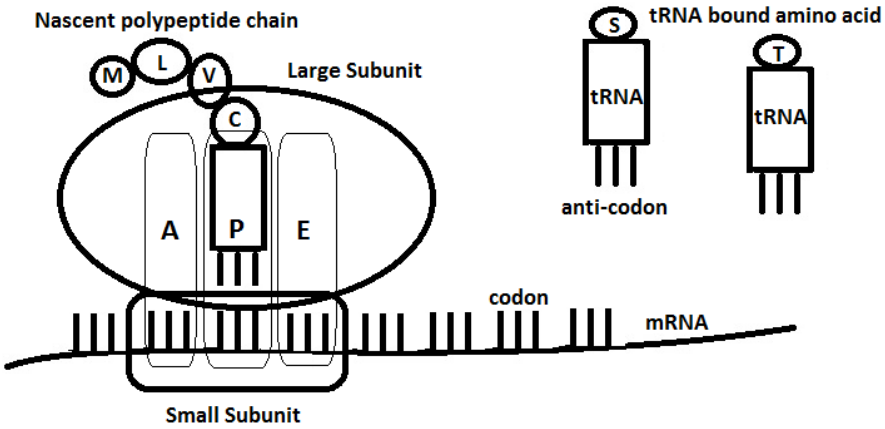

Figure 2.1. Schematic representation of translation mechanism.

between the amino acid bound to the peptidyl tRNA which stands in P site and amino acid of this aminoacyl tRNA which stands in A site. The uncharged tRNA moves to the E site where it exits the ribosome and the peptidyl tRNA moves from A site to P site. During these processes GTP is hydrolyzed into GDP. One GTP is hydrolyzed during the release of amino acid tRNA complex from EF-Tu GTP complex and then tRNA binds to the A site. Another GTP molecule is hydrolyzed during translocation of tRNA from A site to the P site. GTP molecule bound to the EF-G is hydrolyzed into the GDP during this process [16-18].

2.1.1. Ribosome and RNA Structures

An *E.coli* tRNA molecule bound to cysteine [19] (red spheres) is shown in Figure 2.2. tRNA 3'-CCA acceptor ends carry these amino acids, and the growing polypeptide chain [20].

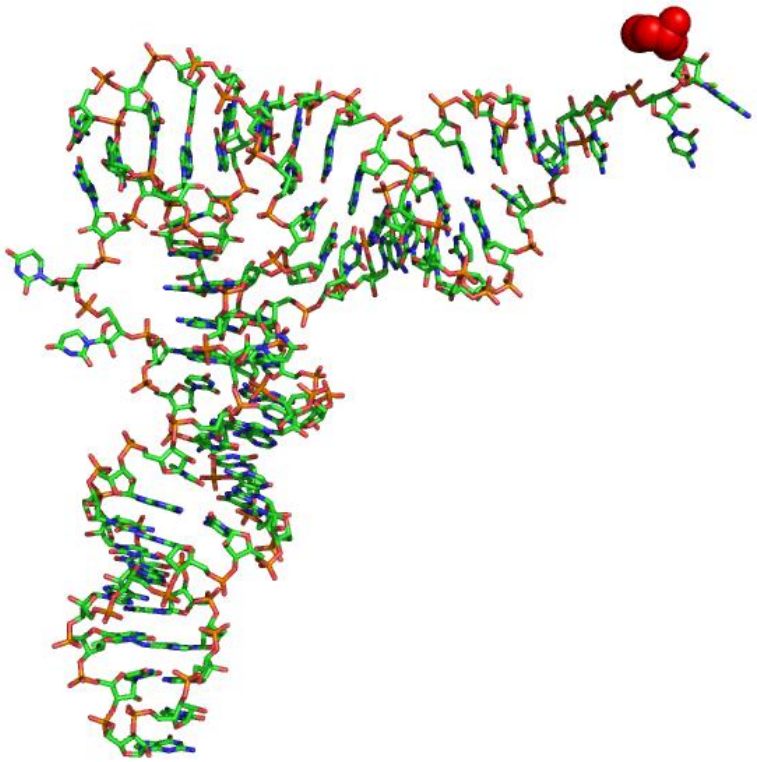

Figure 2.2. tRNA molecule bound to cysteine.

The structure of ribosome is formed with rRNA and ribosomal proteins. The structure of *T. thermophilus* 50S ribosome (Protein Data Bank [21] (PDB): 1GIY) [20] is shown in Figure 2.3. The orange molecules represent 23S and 5S rRNA atoms and yellow molecules are the ribosomal proteins. The landmarks of the structure such as L1 stalk, L7/L12 stalk, body and center protuberance (CP) are shown in this figure. The structure of *E. coli* 50S (PDB: 2AW4) and 30S ribosome subunit (PDB: 2AVY) [22] structures are shown in Figure 2.4. In Figure 2.4a, the ribosome structure including both 50S and 30S structures is shown according to the landmarks shown in Figure 2.3. In Figure 2.4b, the structure is rotated 90 ^{o}C so that the 50S (23S rRNA: grey, 50S ribosomal proteins: cyan) and 30S (16S rRNA: orange, 30S ribosomal proteins: magenta) subunits are apparent.

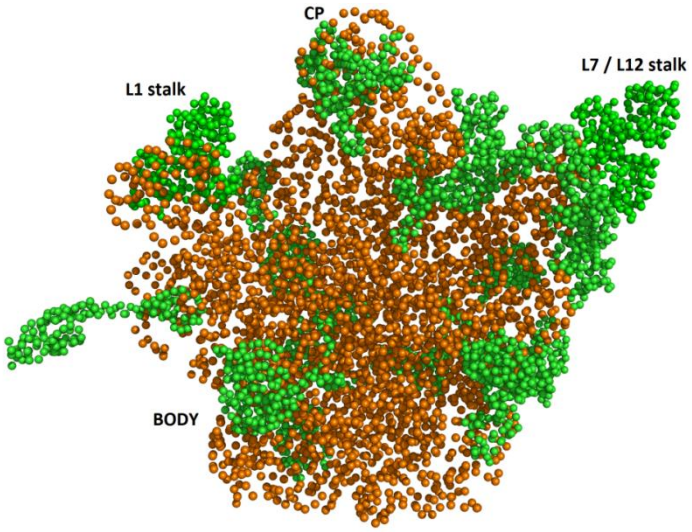

Figure 2.3. *T. thermophilus* 50S ribosome structure.

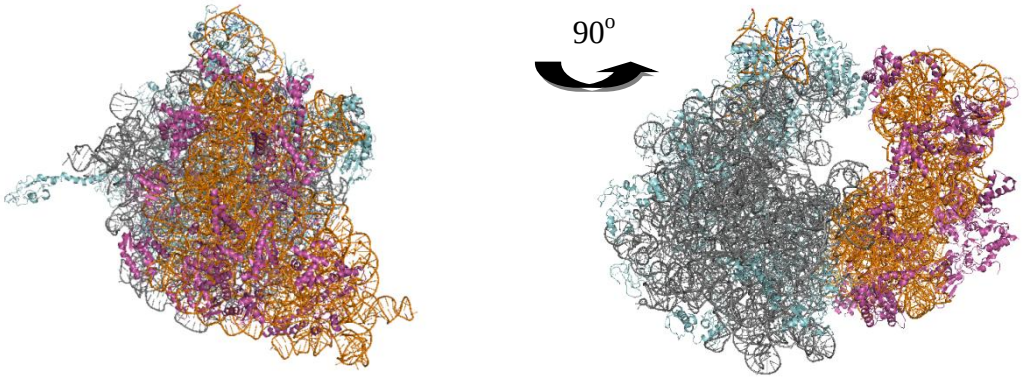

Figure 2.4. The structure of *E. coli* ribosome (50S and 30S subunits).

The initiation complex (PDB: 2HGR, 2HGU) including a $tRNA^{fMet,}$ $tRNA^{Phe}$ and mRNA sequence is given in Figure 2.5. The post-initiation complex (PDB: 2HGP, 2HGQ) with three $tRNA^{Phe}$ molecules is shown in Figure 2.6 [23].

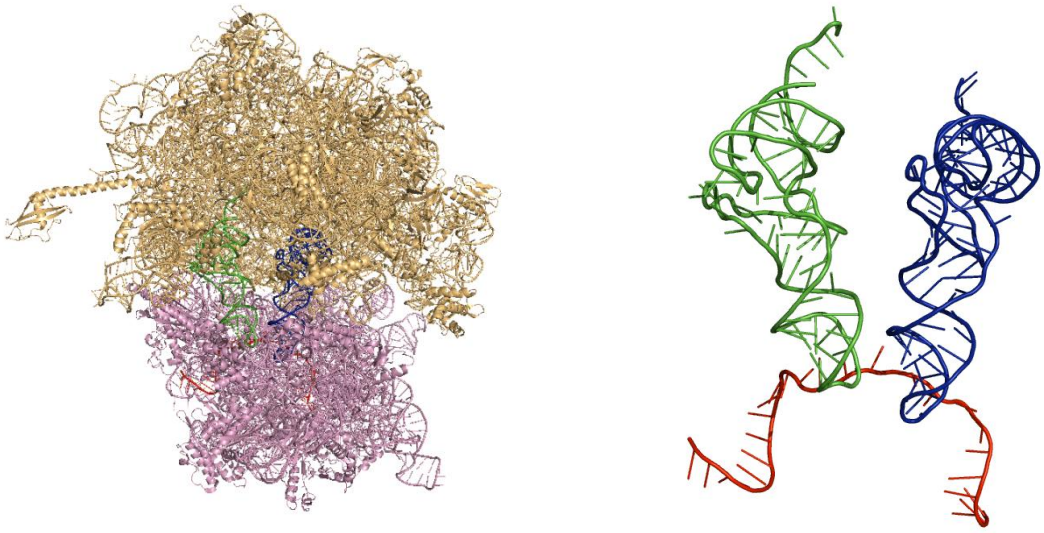

Figure 2.5. The structure of *T. thermophilus* ribosome initiation complex.

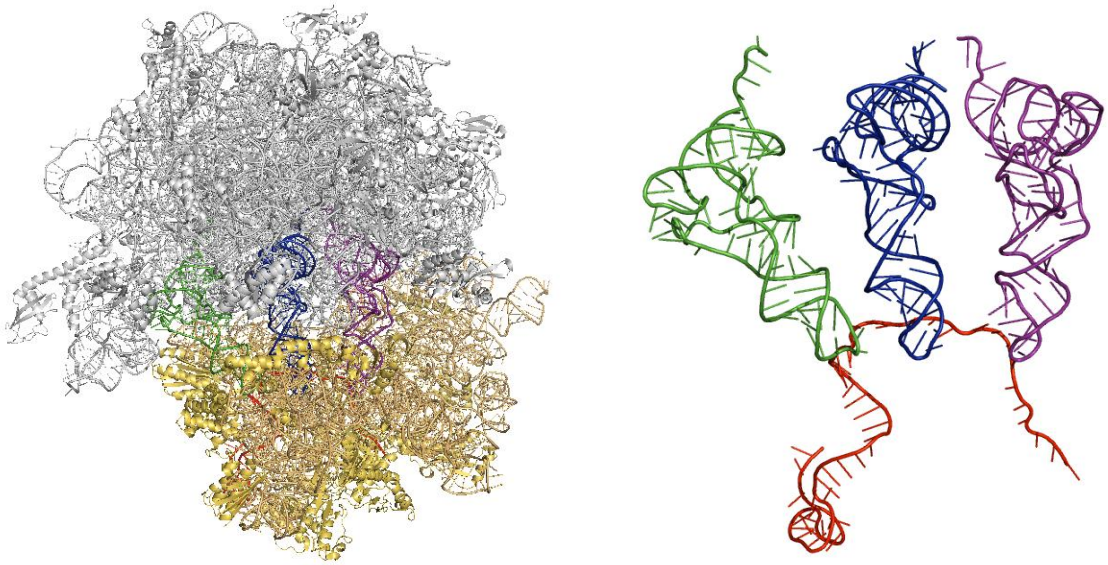

Figure 2.6. The structure of *T. thermophilus* ribosome post-initiation complex.

2.1.2. Secondary Structure of rRNA

The secondary structures of *E. coli* 23S rRNA – 5’ half, 23S rRNA – 3’ half and 16S rRNA are given in Figure 2.7-2.9 [24]. 6 domains of 23S rRNA is given in Figure 2.7, 2.8. Antibiotics mostly bind to the domain V and sometimes to the domains II and IV [4, 8, 25].

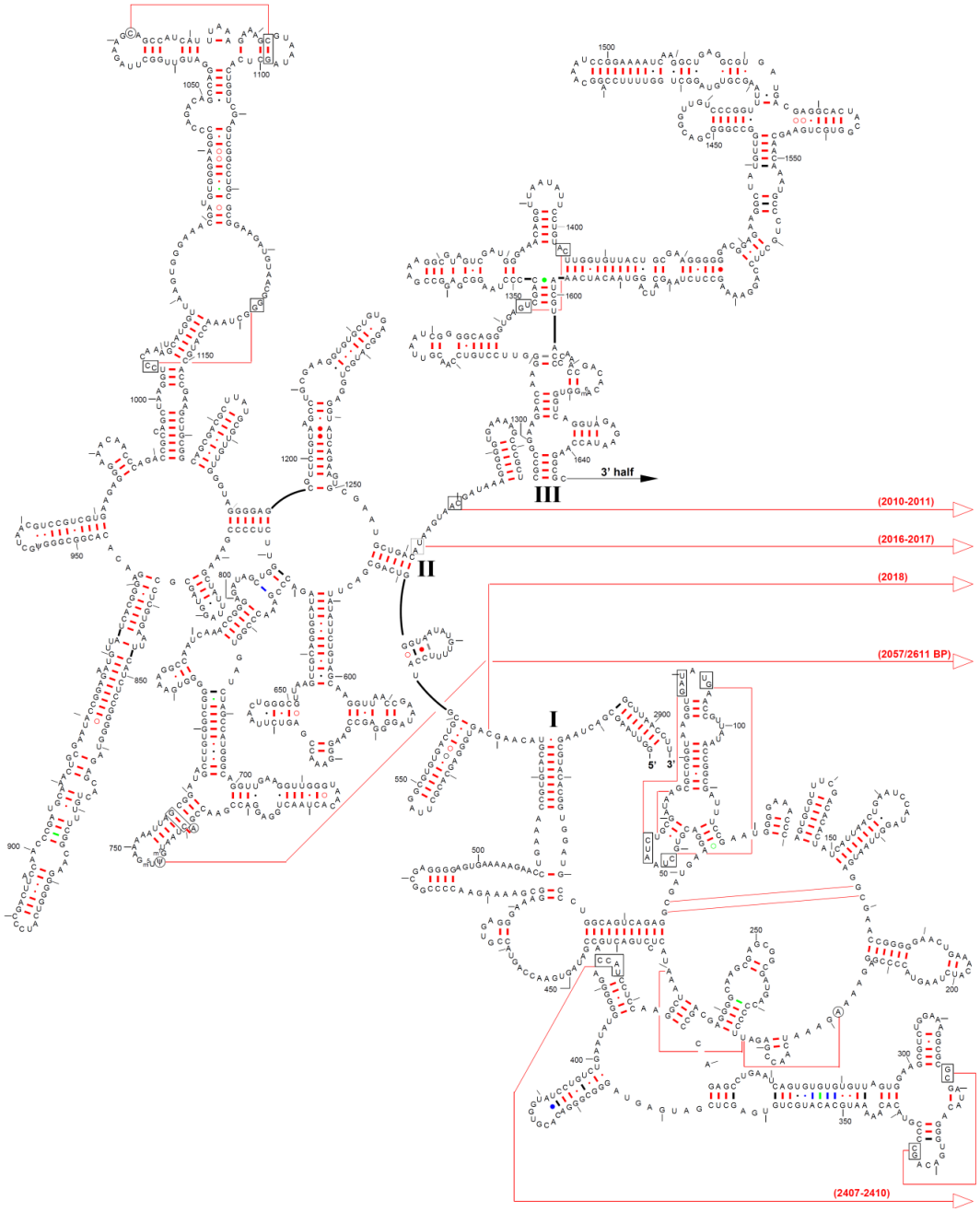

Figure 2.7. The secondary structure of *E. coli* 23S rRNA – 5’ half.

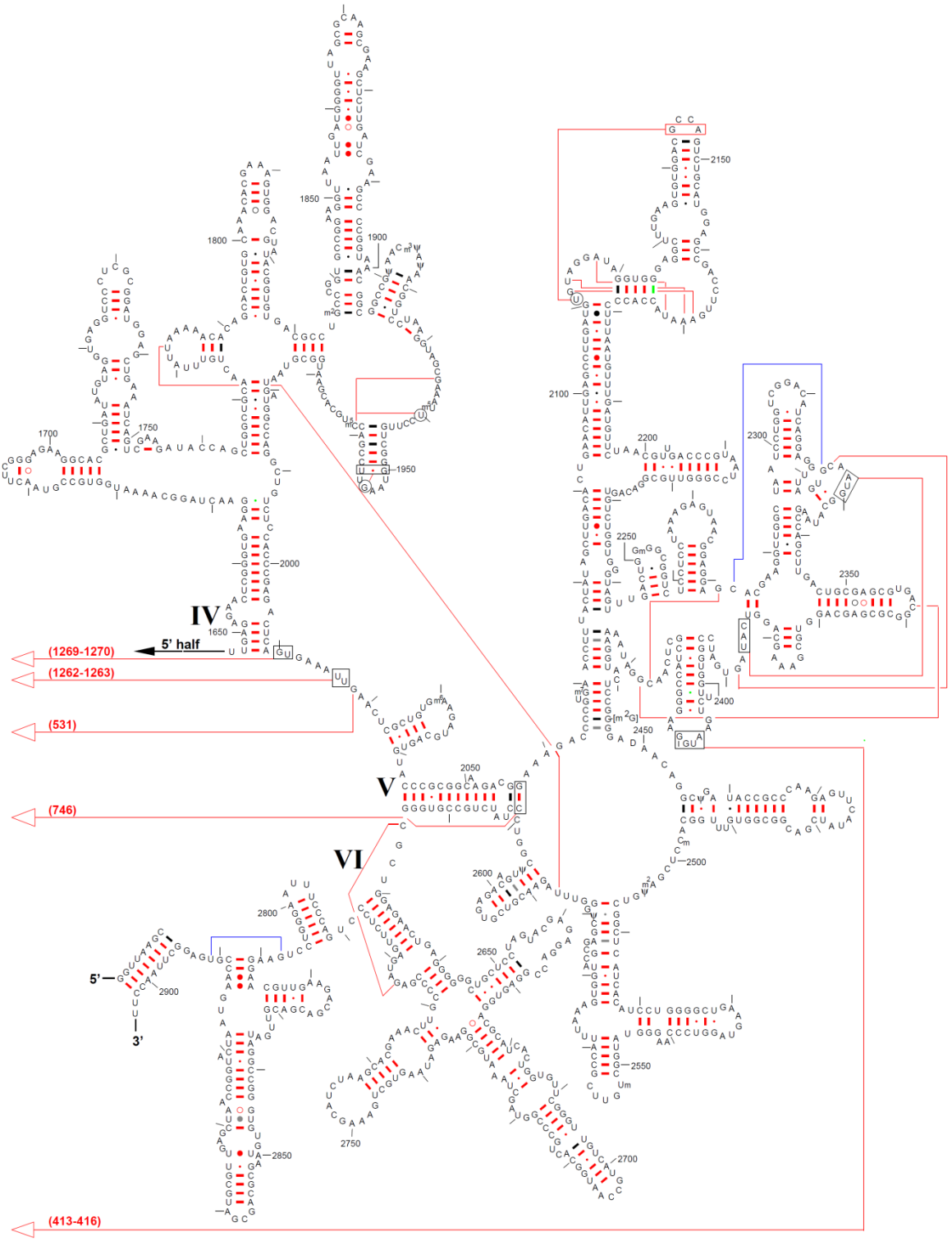

Figure 2.8. The secondary structure of *E. coli* 23S rRNA – 3' half.

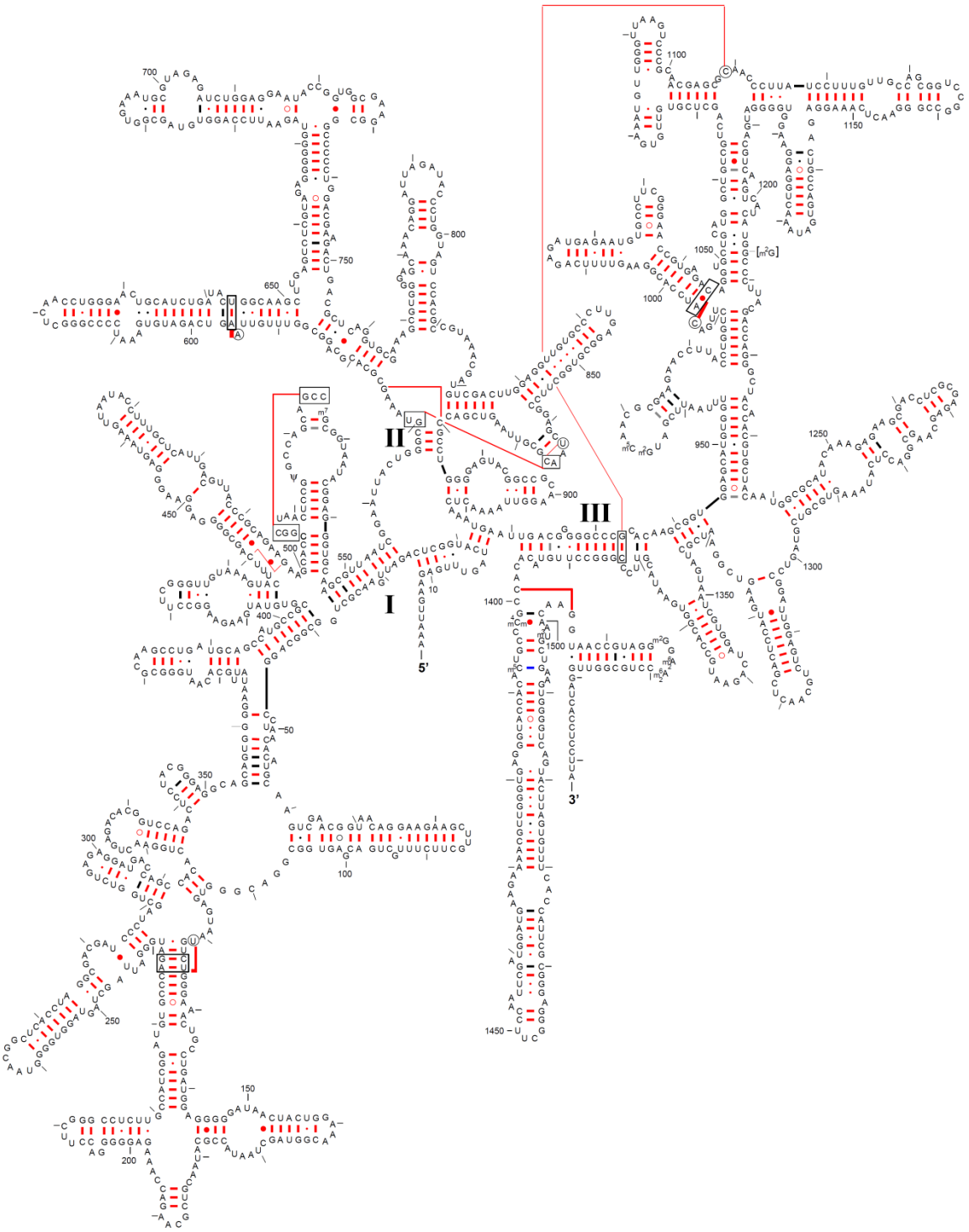

Figure 2.9. The secondary structure of *E. coli* 16S rRNA.

2.2. Antibiotics

Ancient cultures were using plant extracts for infectious diseases. After the discovery of microorganisms and their structures several ways to block their living cycle have been searched. These studies give rise to a new kind of drug, antibiotics. The pioneering study which is resulted in the discovery of penicillin was carried out by Alexander Fleming. The effect of penicillin on *E.coli* growth is shown in Figure 2.10. *E.coli* culture was cultivated in a Petri dish after a drop of penicillin was poured in the middle of that Petri dish. It is obvious that the area containing penicillin inhibit the growth of microorganisms. Other parts show well grown colonies. The natural antibiotics such as penicillin which is obtained from the Penicillium kind of fungi, synthetic and semi-synthetic antibiotics are mostly used to treat infectious diseases. However, the development of new class of antibiotics and finding the functional derivatives of existing ones are a necessity since microorganisms gain resistance by mutations in their genetic material and conformational rearrangements in their structures.

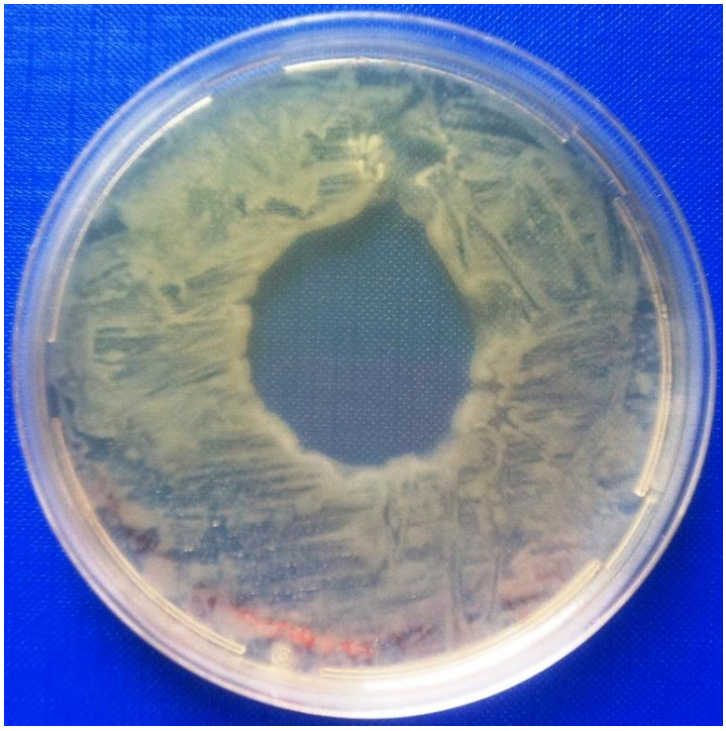

Figure 2.10. Effect of penicillin on *E.coli* growth.

One of the ways to kill the microorganisms by antibiotics is to inhibit phosphorylation like oligomycin [26]. One of the major class of antibiotics interferes with the synthesis of bacterial cell wall polysaccharides, peptidoglycans. The antibiotics bacitracin and vancomycin are good examples as inhibitors of bacterial cell wall synthesis reactions [16]. The structure of vancomycin which is an asymmetric dimer (PDB: 1SHO) is shown in Figure 2.11 [27].

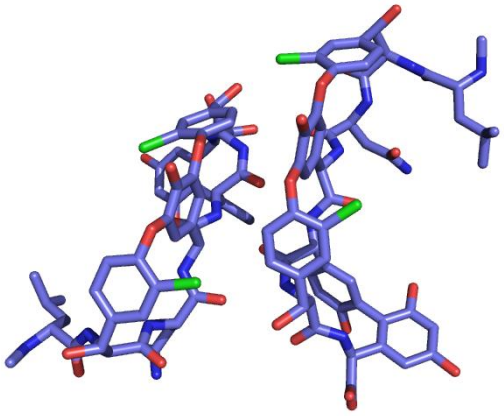

Figure 2.11. The structure of vancomycin.

The specificity of antibiotics is another important issue that has to be considered to be used as an effective drug. As expected, antibiotics should inhibit only pathogenic microorganisms. The host cells should not be affected by these drugs. The targeted antibiotics that only affect the pathogenic bacteria without the beneficial ones for the host are even more important. Therefore, it is better to design species specific drugs. The broad spectrum antibiotics are generally nonspecific drugs that may also kill host cells. In order to overcome this disadvantage, a new class of antibiotics had been synthesized. Generally, antibiotics that block cell wall, peptidoglycan, or cell membrane are broad spectrum antibiotics.

The narrow spectrum antibiotics which are species specific could be developed by blocking the protein synthesis in ribosomes. The reason is that those kinds of antibiotics almost always interact with rRNA. This approach takes advantage of the species specific nucleotide sequence. This kind of antibiotics includes macrolides, ketolides which are semi-synthetic derivatives of macrolides, lincosamides and tetracyclines.

2.3. Allostery in Ribosome

Allostery (allos “other,” steros “space”) is the idea of communication of one site in biological molecules with another site. These sites may be close or distal to each other. Therefore neighboring nucleotides in the antibiotics binding sites may also be critical for the affect of antibiotics and ribosome activity. These nucleotides are the second shell nucleotides. In 23S rRNA some of these nucleotides are reported as the nucleotides that affect the interaction with antibiotics [10, 28]. These remote interactions form a network as in the case of lankacidin which is a polyketide antibiotic. It is produced by *Streptomyces rochei* and it binds to the PTC of eubacterial 50S subunit (PDB: 3JQ4). Second shell nucleotides for lankacidin case are 2576 (2555), 2062 (2045), 2530 (2509), 2531 (2510), 2507 (2486), 2584 (2563), 2581 (2560), 2610 (2589), and 2059 (2042). Nucleotides in parenthesis are numbered according to *D. radiodurans* structure.

Mutations in second shell nucleotides may cause resistance of the antibiotics allosterically even they are not in the binding sites [10]. 23S rRNA nucleotide 2062 E.c. (2045 D.r.) is one of these neighboring nucleotides which affects the binding of chloramphenicol to the eubacterial large subunit by mutation (PDB: 1K01) [1]. Linezoid, oxazolidinone class of antibiotics, binding is also affected allosterically by the mutations at the adjacent bases of binding sites probably by perturbing the base 2504 E.c. (2483 D.r.) [10]. Majority of the mutations targeting the bases in the vicinity of the PTC does not interact with the bound compound directly, but they are in an interaction network with PTC nucleotides [29].

Ribosomal proteins also take role in the antibiotics binding affinity. Especially the nascent polypeptide chain exit tunnel is important in this mechanism since its wall is constituted also by ribosomal proteins L4, L22, L23 (superposes well with L39 in archaebacteria *H. marismortui*) and L32 [1-3, 25]. Mutations in these proteins perturb the rRNA and form resistance although they are not enough close to the ligand for a meaningful chemical interaction [1].

3. METHODS

3.1. Gaussian Network Model

The ribosome structure dataset studied in this thesis are mainly constructed on a combination of two datasets for 4 different microorganisms reported by Wilson, N.W [18] and Mandel-Gutfreund [15] considering either only antibiotics bound or unbound structures. The structures are given in Table 3.1 including their crystallographic data references.

Gaussian Network Model (GNM) idea comes from the Elastic Network Model which was proposed by Tirion [30]. GNM, originally proposed by Bahar *et al*. [31, 32], is a network of residues considered as nodes connected by virtual springs. Starting point is a stable conformation that represents the minimum of the potential energy surface. The harmonic approximation of the potential well was constructed around this conformation. The springs connecting these nodes within a cutoff distance, r_c, are representative of the bonded and non-bonded interactions. Schematic representation of GNM, where the equilibrium positions of ith and jth nodes and the virtual springs connecting the nodes are represented, is shown in Figure 3.1 [33].

The fluctuations are assumed to be isotropic and Gaussian so that the potential can be written as

$$V_{GNM} = \frac{\gamma}{2}\left[\sum_{i,j}^{N} \Gamma_{ij}\left[\left(\Delta X_i - \Delta X_j\right)^2 + \left(\Delta Y_i - \Delta Y_j\right)^2 + \left(\Delta Z_i - \Delta Z_j\right)^2\right]\right] \qquad (3.1)$$

where γ is the force constant and Γ_{ij} is the element of Kirchhoff (connectivity) matrix defined by Equation 3.2 [31-33].

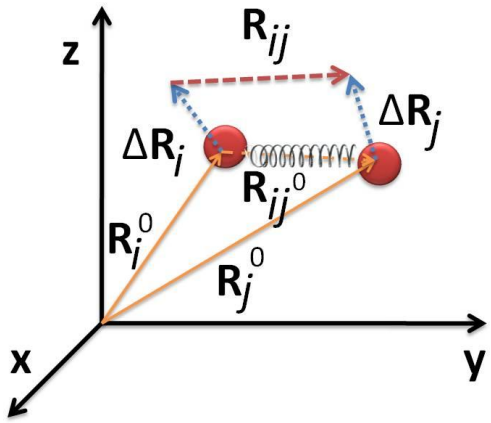

Figure 3.1. Schematic representation of GNM. $\mathbf{R_i^o}$ represents the equilibrium position vector and $\mathbf{R_i}$ is the instantaneous position vector of ith residue. The fluctuation is given by $\mathbf{\Delta R_i = R_i - R_i^o}$.

$$\Gamma_{ij} = \begin{pmatrix} -1 & \text{if } i \neq j \text{ and } R_{ij} \leq r_c \\ 0 & \text{if } i \neq j \text{ and } R_{ij} > r_c \\ -\sum_{j,j\neq i} \Gamma_{ij} & \text{if } i = j \end{pmatrix} \tag{3.2}$$

Application of GNM to free and enzyme-bound tRNA molecule was applied by Bahar and Jernigan [34]. For the free tRNA molecule, one interaction site was selected which is located at the phosphorus atom represents each nucleotide. For the enzyme-bound tRNA, two interaction sites located at the P and O_4 atoms were used and the r_c was taken between 16-19 Å according to the complex structure. In this study, we use different r_c values (10 Å, 16 Å, 20 Å) for optimization. GNM simulations with 20 Å r_c give best results.

The correlation $\langle \Delta \mathbf{R}_i \cdot \Delta \mathbf{R}_j \rangle$ between the fluctuations of residues i and j will be evaluated from;

$$\langle \Delta \mathbf{R}_i \cdot \Delta \mathbf{R}_j \rangle = \frac{3}{2} (\mathbf{\Gamma}^{-1})_{ij} = \frac{3}{2} \sum_k \lambda_k^{-1} (\mathbf{u}_k)_i (\mathbf{u}_k)_j \tag{3.3}$$

where, λ_k and $\mathbf{u}_k$ are the kth nonzero eigenvalue and corresponding normalized eigenvector of the connectivity matrix, respectively. Relative fluctuations $\langle \Delta\mathbf{R}_{ij}{}^2 \rangle \equiv \langle \left(\Delta\mathbf{R}_i - \Delta\mathbf{R}_j\right)^2 \rangle$ are calculated as;

$$\langle \Delta\mathbf{R}_{ij}{}^2 \rangle = \langle \Delta\mathbf{R}_i{}^2 \rangle - 2\langle \Delta\mathbf{R}_i \cdot \Delta\mathbf{R}_j \rangle + \langle \Delta\mathbf{R}_j{}^2 \rangle \tag{3.4}$$

$$\langle \Delta\mathbf{R}_{ij}{}^2 \rangle = \sum_k \lambda_k^{-1} \left[(\mathbf{u}_k)_i{}^2 - 2(\mathbf{u}_k)_i (\mathbf{u}_k)_j + (\mathbf{u}_k)_j{}^2 \right] \tag{3.5}$$

$\langle \Delta\mathbf{R}_{ij}{}^2 \rangle$ gives information about the correlation and the mobilities of the residues. The high frequency fluctuating nucleotides are the nucleotides that display the highest mean distance fluctuations in the high frequency mode. Analysis of fast modes gives local behavior whereas slow modes give global motions and cooperativity [35-37]. In this study since the objective is to find the antibiotic binding sites in ribosomes we focus on the fast modes.

The results are also reported in terms of sensitivity (SN), specificity (SP), precision (PRE) and accuracy (ACC), based on the following definitions where TP, TN, FP and FN represent the number of true positives, number of true negatives, number of false positives and number of false negatives, respectively [36].

$$\mathrm{SN} = \frac{\mathrm{TP}}{\mathrm{FP} + \mathrm{FN}} \tag{3.6}$$

$$\mathrm{SP} = \frac{\mathrm{TN}}{\mathrm{FP} + \mathrm{TN}} \tag{3.7}$$

$$\mathrm{PRE} = \frac{\mathrm{TP}}{\mathrm{TP} + \mathrm{FP}} \tag{3.8}$$

$$\mathrm{ACC} = \frac{\mathrm{TP} + \mathrm{TN}}{\mathrm{TP} + \mathrm{FP} + \mathrm{TN} + \mathrm{FN}} \tag{3.9}$$

Secondary structure diagram is constructed by VARNA applet [38] based on the data given by Gutell R.R.'s study on the database of comparative sequence and structure information for ribosomal, intron and other RNAs [24].

3.2. Z-Score Analysis

The probability of a result *x* in an experiment with enough large number of independent trials is approximated by normal (Gaussian) distribution. It has a bell-shaped probability density function. Z-score which is also called as the standard score gives information about the number of standard deviations from mean at each residue. It is a standardization (normalization) process of the data to make them possible to compare between different experiments. It is not possible otherwise, since mean value and standard deviation depend on the number of trials in the experiment. Z score is defined in Equation 3.10.

$$\mathrm{Z}_i = \frac{\mathrm{r}_i - \bar{\mathrm{r}}_i}{\sigma} \tag{3.10}$$

Here, Z_i is the Z-score of ith predicted residue. r_i is the closest distance between the predicted residue *i* and the experimentally known binding sites. $\bar{r}_i$ is the mean distance of all residues with the binding site that is closest to the ith residue and σ is the corresponding standard deviation [39]. *Z* is negative when r_i is below the mean distance $\bar{r}_i$ and positive when above. A predicted residue will have smaller Z-score when it is close to the binding site. For each fast mode mean Z-score is calculated to make a comparison between them and between different cases.

Title 3.1. Antibiotics bound and unbound crystallographic structures.

Index	Organism	Subunit	PDB	Antibiotics	Reference
1	D.r	23S	1J5A	Clarithromycin	[1]
2	D.r	23S	1JZX	Clindamycin	[1]
3	D.r	23S	1JZY	Erythromycin	[1]
4	D.r	23S	1JZZ	Roxithromycin	[1]
5	D.r	23S	1K01	Chloramphenicol	[1]
6	D.r	23S	1NJN	Sparsomycin	[14]
7	D.r	23S	1NKW	Unbound	[40]
8	D.r	23S	1NWX	ABT-773	[2]
9	D.r	23S	1NWY	Azithromycin	[2]
10	D.r	23S	1OND	Troleandomycın	[3]
11	D.r	23S	1P9X	Telithromycin	[8]
12	D.r	23S	1SM1	Quinupristin, Dalfopristin	[13]
13	D.r	23S	1XBP	Tiamulin	[12]
14	D.r	23S	1Z58	Rapamycin	[25]
15	D.r	23S	2O43	Erythromycylamine	[4]
16	D.r	23S	2O44	Josamycin	[4]
17	D.r	23S	2O45	Ru-69874	[4]
18	D.r	23S	2OGM	SB-571519	[29]
19	D.r	23S	2OGN	SB-280080	[29]
20	D.r	23S	2OGO	SB-275833	[29]
21	D.r	23S	2ZJP	Nosiheptide	[41]
22	D.r	23S	2ZJR	Unbound	[41]
23	D.r	23S	3CF5	Thiostrepton	[41]
24	D.r	23S	3DLL	Oxazolidinone	[10]
25	D.r	23S	3FWO	Methymycin	[5]
26	D.r	23S	3JQ4	Lankacidin	[28]
27	E.c	16S	1VS5	Kasugamyin	[42]
28	E.c	16S	2AVY	Unbound	[22]
29	E.c	16S	2QAL	Neomycin	[17]
30	E.c	16S	2QB9	Gentamicin	[17]
31	E.c	16S	2QOU	Spectinomycin	[43]
32	E.c	16S	3DF1	Hygromycin B	[44]
33	E.c	16S	3I1M	Unbound	[45]
34	E.c	23S	2AW4	Unbound	[22]
35	E.c	23S	2QOZ	Neomycin	[43]
36	E.c	23S	3OAT	Telithromycin	[6]
37	E.c	23S	3OFC	Chloramphenicol	[6]
38	E.c	23S	3OFR	Erythromycin	[6]

Title 3.1. Antibiotics bound and unbound crystallographic structures, cont.

Index	Organism	Subunit	PDB	Antibiotics	Reference
39	E.c	23S	3OFZ	Clindamycin	[6]
40	E.c	23S	3ORB	CEM-101	[9]
41	E.c	23S	3I1N	Unbound	[45]
42	H.m	23S	1JJ2	Unbound	[46]
43	H.m	23S	1K73	Anisomycin	[47]
44	H.m	23S	1K8A	Carbomycin A	[7]
45	H.m	23S	1K9M	Tylosin	[7]
46	H.m	23S	1KC8	Blasticidin S	[47]
47	H.m	23S	1KD1	Spiramycin	[7]
48	H.m	23S	1M1K	Azithromycin	[7]
49	H.m	23S	1N8R	Virginiamycin M	[47]
50	H.m	23S	1NJI	Chloramphenicol	[47]
51	H.m	23S	1YIT	Virginiamycin M, Virginiamycin S	[48]
52	H.m	23S	2OTJ	13-Deoxytedanolide	[49]
53	H.m	23S	2OTL	Girodazole	[49]
54	H.m	23S	3CC4	Anisomycin	[50]
55	H.m	23S	3G4S	Tiamulin	[51]
56	H.m	23S	3G6E	Homoharringtonine	[51]
57	H.m	23S	3G71	Bruceantin	[51]
58	H.m	23S	3I55	Mycalamide A	[52]
59	H.m	23S	3I56	Triacetyloleandomcyin	[52]
60	T.t	16S	1FJG	Paromomycin, Spectinomycin, Streptomycin	[53]
61	T.t	16S	1HNW	Tetracycline	[54]
62	T.t	16S	1HNX	Pactamycin	[54]
63	T.t	16S	1HNZ	Hygromycin B	[54]
64	T.t	16S	1I95	Edeine	[55]
65	T.t	16S	1I97	Tetracycline	[55]
66	T.t	16S	1IBK	Paromomycin	[56]
67	T.t	16S	1J5E	Unbound	[57]
68	T.t	16S	2HHH	Kasugamyin	[58]
69	T.t	23S	1GIY	Unbound	[20]
70	T.t	23S	3OH5	Chloramphenicol	[59]
71	T.t	23S	3OHJ	Erythromycin	[59]
72	T.t	23S	3OI1	Azithromycin	[59]
73	T.t	23S	3OI3	Telithromycin	[59]

4. RESULTS AND DISCUSSION

4.1. Alignment of Large Subunit Antibiotics Binding Sites

During the analysis of antibiotics binding sites, the experimental data extracted from the biochemical and crystallographic data given for each antibiotics bound complex in Table 3.1 were compared with high frequency fluctuating residues by the GNM analysis. Also, the theoretical binding sites are defined according to the closest distance of a nucleotide's atoms with any atom of the antibiotics. If the closest distance is less than 6 Å, it is defined as a theoretical binding site [15]. The GNM predictions are also compared with these sites.

The antibiotics binding sites in both 50S and 30S ribosomal subunits are compared by aligning structures. All four microorganisms, *D. radiodurans*, *E. coli*, *H. marismortui* and *T. thermophilus* have antibiotics bound 50S structures, but only *E. coli* and *T. thermophilus* have antibiotics bound 30S structures in Table 3.1. There are totally 64 antibiotics bound structures and 9 of these structures were crystallized with more than one antibiotics. One *T. thermophilus* 30S structure (PDB: 1FJG) and one *E. coli* 30S structure (PDB: 2QB9) have 3 antibiotics. A *T. thermophilus* 30S structure (PDB: 1I97) has even 5 tetracycline antibiotics bound to it. These structures may include same kind of antibiotics as in 2QB9 structure with 3 gentamycin or different kinds of antibiotics as in 1FJG structure with paromomycin, spectinomycin and streptomycin. 1NWY, 1SM1, 1KC8, 1YIT, 1HNW and 2HHH are ribosome structures having 2 antibiotics.

Each species has also antibiotics unbound structures listed in Table 3.1. Among these unbound structures, 23S *D. radiodurans* structure (PDB: 1NKW) is used to show all the antibiotics that bind to large ribosomal subunits of all these species. Each large subunit structure is aligned with 23S *D. radiodurans* structure (PDB: 1NKW) and their antibiotics coordinates are extracted after structural alignment. In order to realize where these antibiotics bind in these large subunits consisting approximately 2900 nucleotides, A, P, E site tRNAs and mRNA structures are obtained from the 2HGP, 2HGQ PDB files. These

are *T. thermophilus* 30S and 50S structures, respectively. The large ribosomal subunit antibiotics binding sites obtained from these alignments are shown in Figure 4.1.

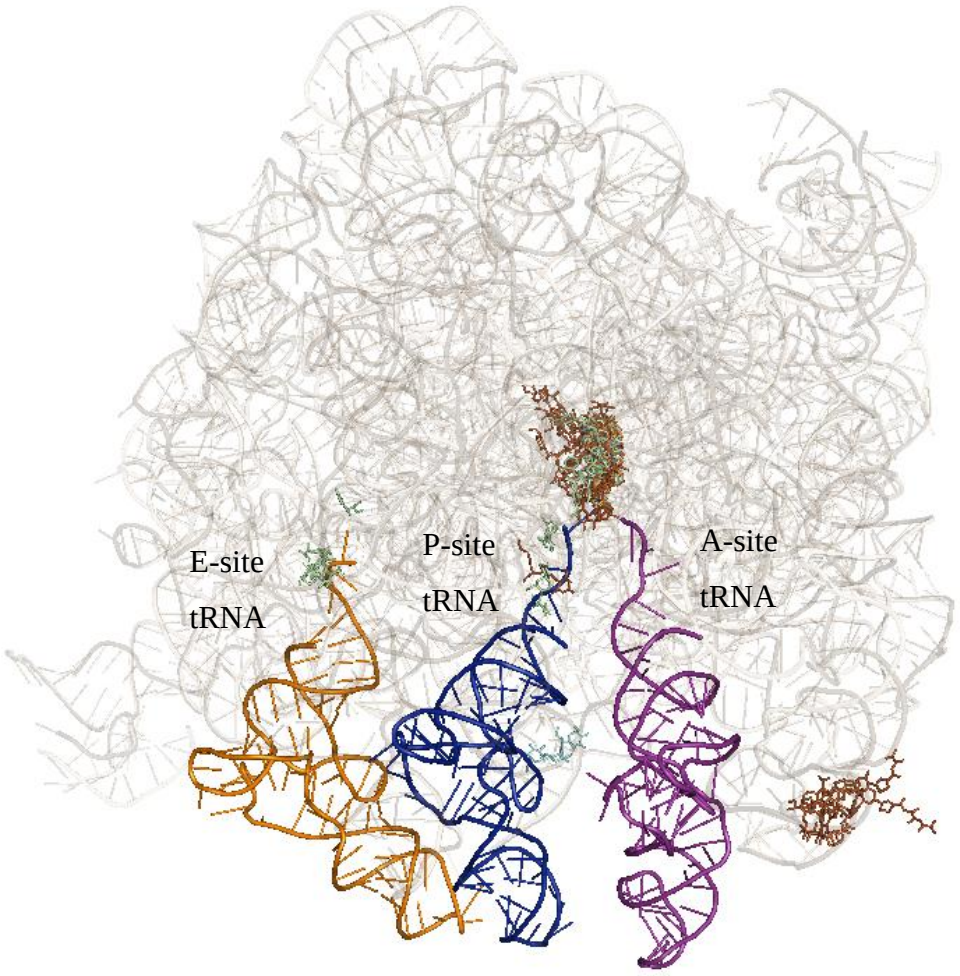

Figure 4.1. Binding sites of antibiotics bound to large ribosomal subunit.

The 23S rRNA and tRNAs are represented in cartoon and antibiotics are represented in sticks in Figure 4.1. For clarity, 23S rRNA is shown in transparent form. The orange, blue and purple molecules are E, P and A site tRNAs, respectively. Antibiotics molecules bound to *D. radiodurans*, *E. coli*, *H. marismortui* and *T. thermophilus* microorganisms are in brown, cyan, green and orange, respectively. Antibiotics bound to each microorganism are given in Figure 4.2 separately for clarity. The Peptidyl Transferase Center (PTC) is the site where amino acids at the end of the 3' CCA tail of the P and A site tRNAs make peptide bond. So, this site is one of the functionally most important sites

throughout the ribosome macromolecule. E site tRNA is far away of PTC which exits the ribosome after leaving its amino acid at PTC. Each tRNA binds to the A site by the help of Ef-Tu molecule and GTP hydrolysis, then it passes to P and E sites, respectively. As it is seen, almost all the antibiotics in 50S subunit binds to the A, P and PTC sites and nascent chain exit tunnel entrance which is close to the PTC. 3 antibiotics bind close to the E site.

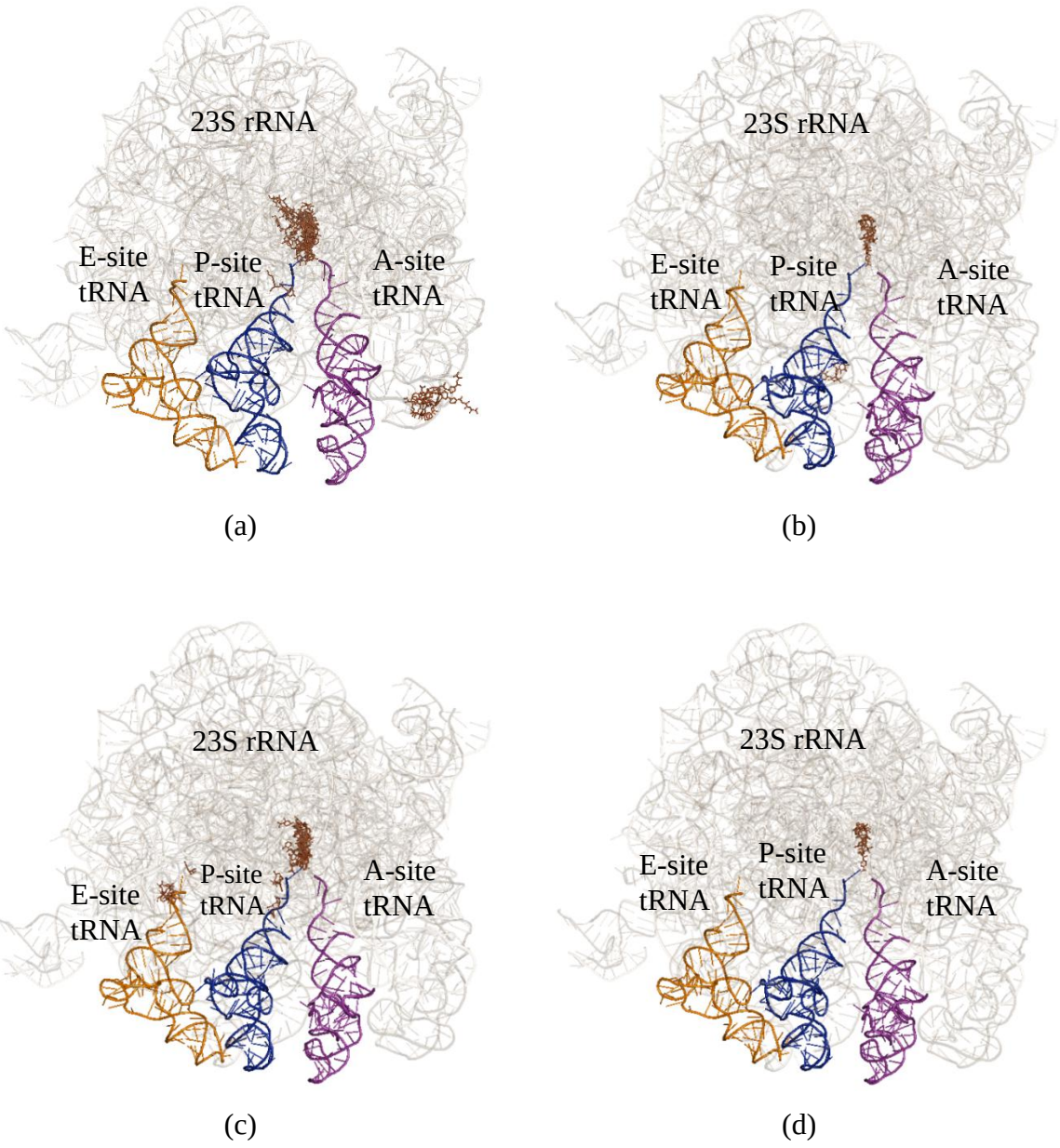

Figure 4.2. Binding sites of antibiotics bound to large ribosomal subunit of (a) *D. radiodurans*, (b) *E. coli*, (c) *H. marismortui* and (d) *T. thermophilus*.

4.2. Nascent Polypeptide Chain Exit Tunnel

Nascent polypeptide chain exit tunnel leads the way to the new grown polypeptide molecules to exit the ribosome. Therefore, this tunnel, especially its entrance, is another key target. The tunnel is shown in Figure 4.3. The blue nucleotides are the nucleotides forming the nascent chain exit tunnel [60]. Orange, pink and green molecules are L4, L22 and L23 ribosomal proteins forming the tunnel.

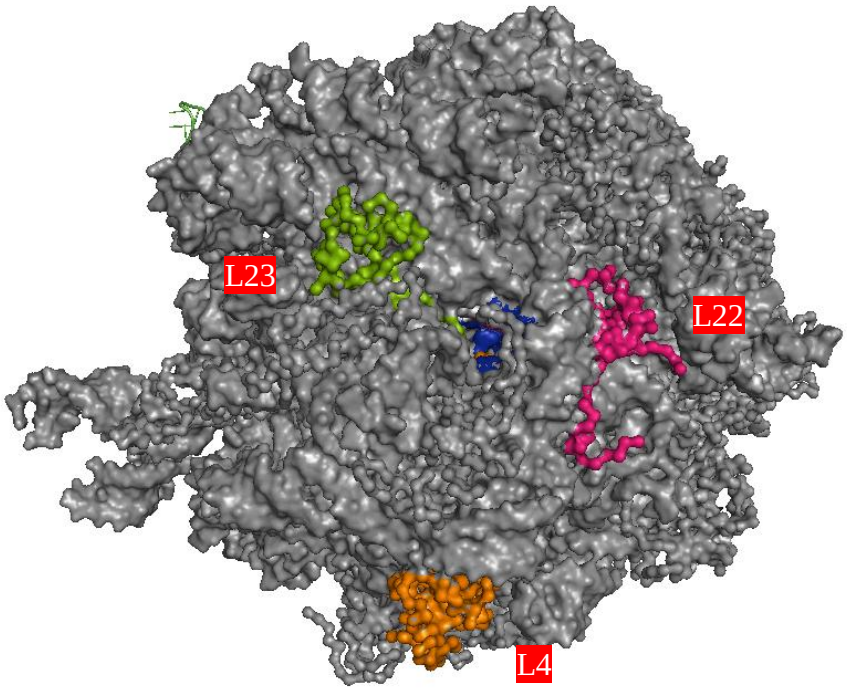

Figure 4.3. Nascent chain exit tunnel surface.

The nascent chain exit tunnel direction is given in Figure 4.4. Exit tunnel starts close to the PTC site where nascent chain is produced. The blue surface starting from the A and P site is formed by the nucleotides of exit tunnel. 30S and 50S subunits of the same ribosome structure (PDB: 2HGP, 2HGQ) are shown in transparent form to visualize the exact location of the exit tunnel. The nucleotides close to the PTC site are more important since they are close to PTC and form the entrance of the exit tunnel. These near neighboring nucleotides are given in blue and nucleotides which are far away of PTC are given in violet in Figure 4.5.

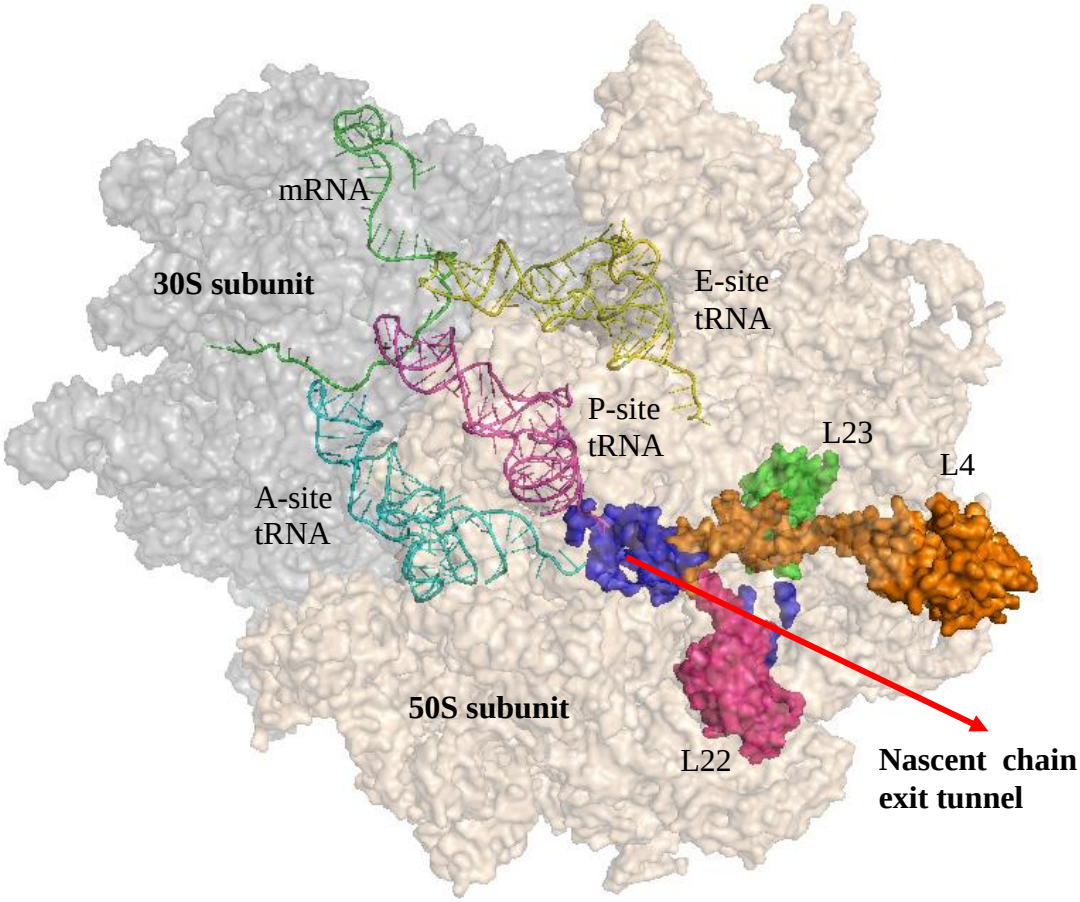

Figure 4.4. Nascent chain exit tunnel direction.

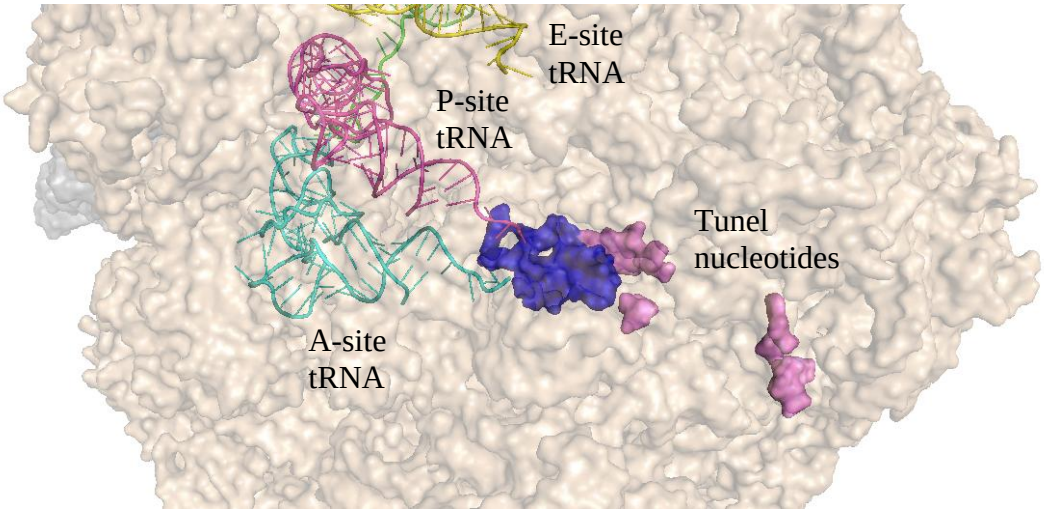

Figure 4.5. Nascent chain exit tunnel nucleotides.

The blue nucleotides in Figure 4.5 are 2041-2045 D.r. (2058-2062 E.c.), 2430 (2451), 2482 (2503), 2484 (2505), 2485 (2506), 2564 (2585), 2565 (2586) and 2581 (2602). Tunnel nucleotides that are not close to PTC (pink nucleotides) are 502 (492), 503 (493), 518 (508), 760 (747), 764 (751), 765 (752), 1334 (1321), 1772 (1781), 1773 (1782) and 2588 (2609). Nucleotide numbering is according to *D. radiodurans* and *E. coli* in parenthesis.

4.3. Alignment of Small Subunit Antibiotics Binding Sites

Most of the antibiotics in Table 3.1 bind to the large subunit of the ribosome. However, antibiotics also target the small subunit. They inhibit protein synthesis by blocking the translocation of tRNAs and mRNA. Small subunit antibiotics bound structures are aligned with the unbound *T. thermophilus* structure (PDB: 1J5E) and shown in Figure 4.6. 16S rRNA is shown in transparent grey. A, P, E-site tRNAs and mRNA are cyan, blue, green and red, respectively. Antibiotics bound to *E. coli* ribosome are shown in purple and others which bind to *T. thermophilus* are shown in orange. They bind to miscellaneous place, but the main targets are tRNA and mRNA sites.

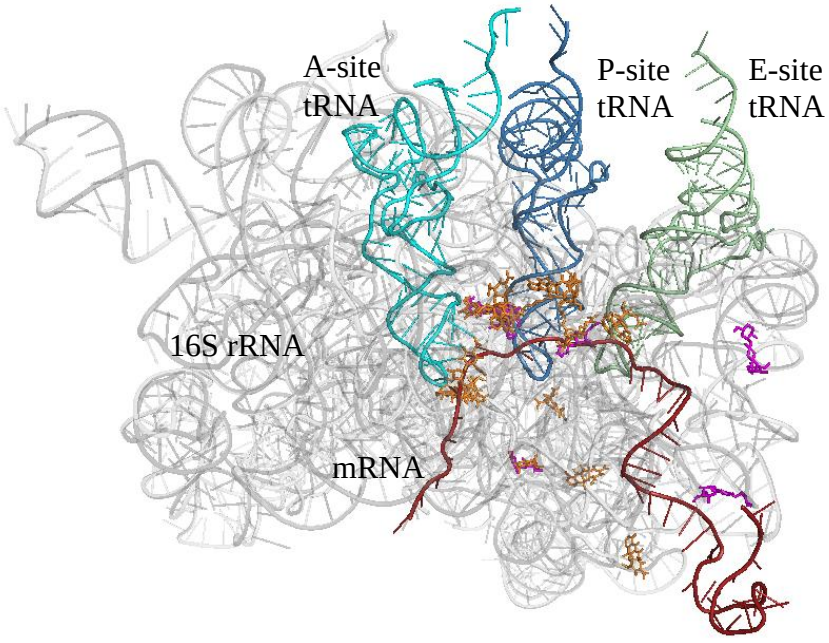

Figure 4.6. Binding sites of antibiotics bound to small ribosomal subunit *E. coli* and *T. thermophilus*.

4.4. Sample Case: Chloramphenicol Binding (PDB: 1K01)

Chloramphenicol binds to the A site and interferes with the binding of tRNA. So, it blocks the peptidyl transferase activity. The structure of chloramphenicol is shown in Figure 4.7. It belongs to macrolide class of antibiotics. The most important nucleotides in the binding of chloramphenicol in *D. radiodurans* are 2044, 2045, 2431, 2483-2485 D.r. which are in the range of hydrogen binding distance and/or they are involved in the antibiotics resistance actions in case of mutations [1].

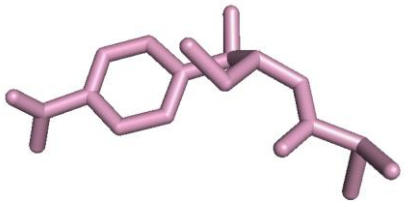

Figure 4.7. Chloramphenicol structure.

The experimental (known) and theoretical binding sites of chloramphenicol are shown in Table 4.1. (nucleotide numbering is based on the *D. radiodurans* structure). The experimental binding sites are extracted from the literature based on the biochemical and crystallographic data. Theoretical binding sites are extracted from the crystallographic data based on the distances between the rRNA nucleotides and antibiotics residues.

GNM is applied to this chloramphenicol bound large ribosomal subunit (PDB: 1K01) and the highest frequency fluctuating nucleotides are selected for the comparison of the antibiotics binding sites based on the total number of the nucleotides having the $<\Delta\mathbf{R}_{ij}^2>$ mean square fluctuation value higher than a threshold. These data are shown in Table 4.2. $<\Delta\mathbf{R}_{ij}^2>$ total count is the cumulative count of $<\Delta\mathbf{R}_{ij}^2>$ counts in second column. It is seen that $<\Delta\mathbf{R}_{ij}^2>$ value of 0.0060 is a threshold at the $<\Delta\mathbf{R}_{ij}^2>$ total count values. There are 50 nucleotide pairs having fluctuation values equal to or greater than 0.0060, but this number jumps to 2765 nucleotide pairs when 0.0050 is taken into account. All the computational data shown in this section belong to the GNM results with 20 Å cut-off distance. Contour map of $<\Delta\mathbf{R}_{ij}^2>$ data of the fastest mode is given Figure 4.8.

Table 4.1. Experimental and theoretical binding sites of chloramphenicol.

Experimental Binding Sites	**Theoretical Binding Sites**
2044	2044
2430	2046
2431	2426
2479	2430
2483	2431
2484	2432
2485	2479
	2482
	2483
	2484
	2485
	2551
	2564
	2581

Table 4.2. $\langle \Delta \mathbf{R}_{ij}^2 \rangle$ mean square fluctuation data counts of fastest mode with 20 Å cut-off value (PDB: 1K01).

$\langle \Delta \mathbf{R}_{ij}^2 \rangle$	$\langle \Delta \mathbf{R}_{ij}^2 \rangle$ **count**	$\langle \Delta \mathbf{R}_{ij}^2 \rangle$ **total count**
0.0090	2	2
0.0080	1	3
0.0070	9	12
0.0060	38	50
0.0050	2715	2765
0.0040	6	2771
0.0030	25	2796
0.0020	2772	5568
0.0010	8337	13905

23S rRNA chain of 1K01 PDB file consists of 2773 nucleotides. Therefore, if 50 nucleotides are selected it means that 1.8% of total number of 23S rRNA nucleotides are selected, which is pretty low value as selected nucleotide percentage.

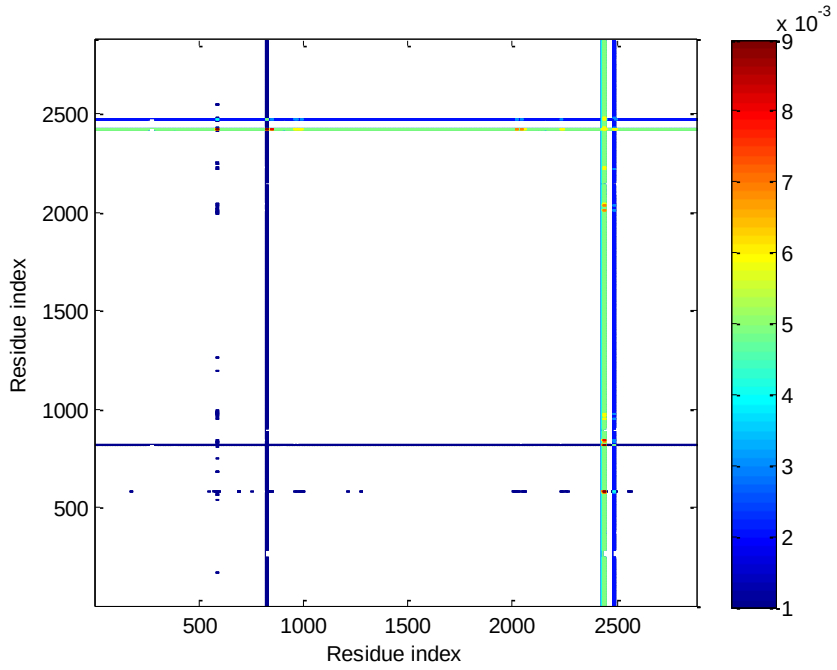

Figure 4.8. Contour map of $<\Delta \mathbf{R}_{ij}^2>$data of the fastest mode.

Binding of chloramphenicol is shown in Figure 4.9. tRNAs and 23S rRNA are shown to clearly define the binding site. Chloramphenicol is shown as pink spheres and the high frequency fluctuating 23S rRNA nucleotides, which are sorted according to the closest distance between the nucleotide and the antibiotics atoms and given in Table 4.3, are shown in surface mode around the antibiotics. It is obvious that high frequency fluctuating nucleotides covers the antibiotics chloramphenicol at the A and P site regions. High frequency fluctuating nucleotides are colored according to the fluctuation values among the selected nucleotides. Red nucleotides are the most fluctuating nucleotides and blue ones are the smallest among the selected highest fluctuating nucleotides. Secondary structure diagram of chloramphenicol binding to the domain V of 23S rRNA of *D. radiodurans* is shown in Figure 4.10. The secondary structure is based on *E. coli* numbering (*D. radiodurans* numbering in parenthesis). The experimentally known binding sites are shown in blue fill color and the predicted binding sites among these are labeled in red.

Table 4.3. High frequency fluctuating nucleotides and distances (PDB: 1K01).

Distance (Å)	**Nucleotide**	**Distance (Å)**	**Nucleotide**
2.232	2430	15.290	2435
2.474	2484	16.749	2012
2.741	2483	18.827	2050
2.958	2044	19.513	843
3.362	2431	19.515	576
4.974	2482	19.669	581
5.015	2432	20.097	2228
6.049	2015	20.262	956
7.058	2038	21.130	973
7.650	2045	21.346	820
8.044	2039	21.444	821
8.748	2433	21.502	974
9.501	2230	22.958	2227
10.036	584	23.804	959
10.697	2476	24.192	958
10.808	583	24.809	957
12.149	2434	25.020	822
12.479	2231	25.638	975
12.747	585	25.643	842
13.091	2475	27.163	844
13.583	2424	28.034	983
13.635	2014	28.739	984
13.996	2427	29.008	955
14.118	2013	30.636	976
15.037	580	30.887	835
15.073	582		

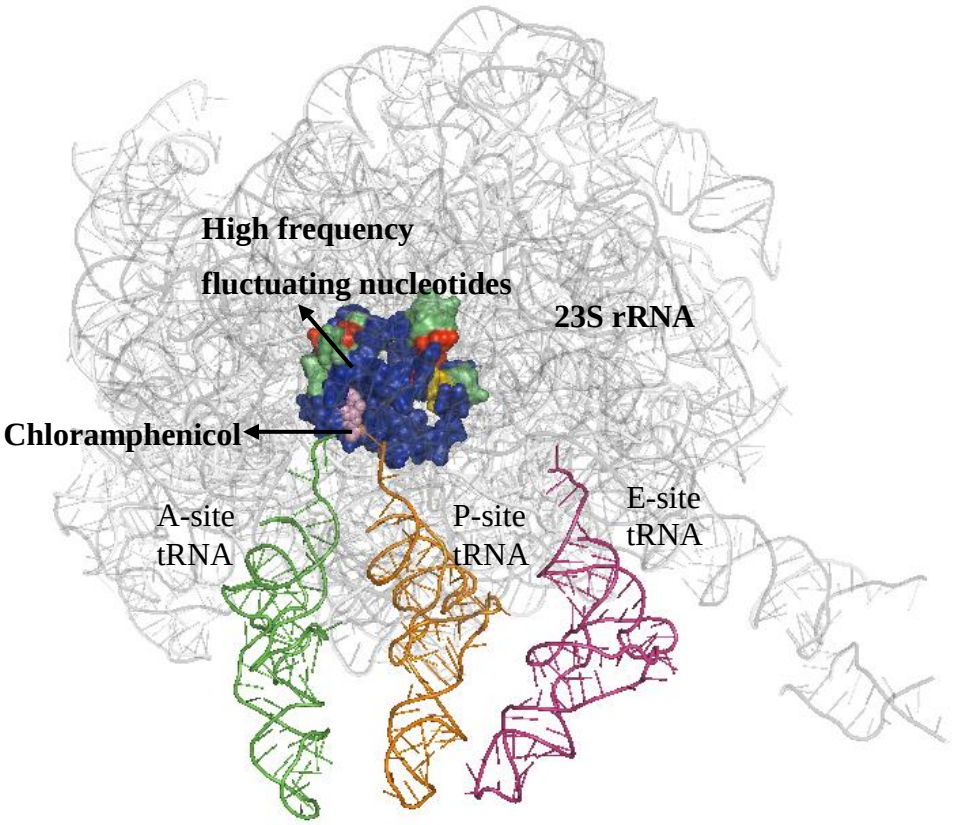

Figure 4.9. Chloramphenicol binding to the 23S rRNA of D.r and high frequency fluctuating nucleotides.

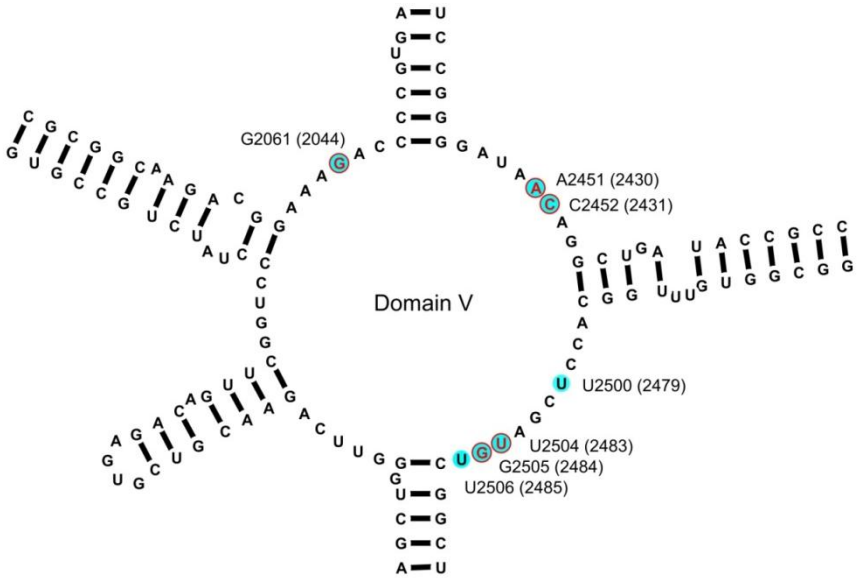

Figure 4.10. Secondary structure diagram of chloramphenicol binding to the domain V of 23S rRNA of D.r.

The experimental and theoretical binding sites of chloramphenicol are shown in Table 4.1. These sites are compared with the high frequency fluctuating nucleotides given in Table 4.3. The high frequency fluctuating nucleotides match accurately with antibiotics binding sites. The important nucleotides for the interaction of antibiotics and 23S rRNA given above are almost completely predicted. Antibotics binding site prediction statistics of GNM based on the experimental binding site data is given in Table 4.4. TP is the true positives. Fast modes are given in the first column. 1_4 and 5_8 are the collective fast modes of modes 1 to 4 and 5 to 8, respectively. There are 7 binding nucleotides experimentally and the fastest mode predicts 5 of these interacting nucleotides. Its sensitivity is 71.4% which is quite satisfactory for this case. Specificity and accuracy are both 98.3%. Precision is 9.8%, but it is due to the number of selected nucleotides. For the first mode totally 51 different nucleotides are selected and there are only 7 experimental binding sites. 5 of these sites are predicted, but it would be 13% even if the all the 7 experimental binding sites are predicted.

Antibiotics binding site prediction statistics of GNM including one neighboring site based on the experimental binding site data for this case is shown in Table 4.5. We know that antibiotics binding nucleotides and their adjacent nucleotides form a network of residues pairs that have high distance fluctuations in fastest modes. Therefore, it is essential to check the neighboring, the second shell nucleotides. Sensitivity is increased to 85.7% from 71.4% since one more binding site nucleotide is predicted compared to the fastest mode in Table 4.4.

High frequency fluctuating nucleotides are also compared with the theoretical binding sites which are determined according to the distance (<6 Å) between the rRNA atoms and antibiotics. Antibiotics binding site prediction statistics of GNM based on the theoretical binding site data is given in Table 4.6 and its statistics including one neighboring base is given in Table 4.7. The binding sites count increases from 7 to 14 when the theoretical binding sites are calculated, but the true positives also increases to 7. These true positives are the first 7 nucleotides having distances lover than 6 Å listed in Table 4.3. Sensitivity is 50%, lower than the sensitivity based on the experimentally known binding sites, but more nucleotides are found close enough to the antibiotics to form strong

chemical interactions. Precision is also increased up to 13.7%. Specificity and accuracy are still almost 100%.

Table 4.4. Antibotics binding site prediction statistics of GNM based on the experimental binding site data (PDB: 1K01).

Fast mode	**Bind sites count**	**TP**	**SN**	**SP**	**PRE**	**ACC**
1	**7**	**5**	**71.4**	**98.3**	**9.8**	**98.3**
2	7	0	0.0	97.7	0.0	97.5
3	7	3	42.9	98.1	5.5	98.0
4	7	1	14.3	98.7	2.7	98.5
1_4	7	2	28.6	98.5	4.6	98.3
5	7	1	14.3	99.1	4.0	98.9
6	7	1	14.3	98.8	3.0	98.6
7	7	1	14.3	98.7	2.6	98.5
8	7	3	42,86	94.6	2.0	94.5
5_8	7	5	71,43	96.9	5.4	96.8

Table 4.5. Antibotics binding site prediction statistics of GNM including one neighboring site based on the experimental binding site data (PDB: 1K01).

Fast mode	**Bind sites count**	**TP**	**SN**	**SP**	**PRE**	**ACC**
1	**7**	**6**	**85.7**	**97.0**	**6.8**	**97.0**
2	7	0	0.0	96.0	0.0	95.7
3	7	5	71.4	96.6	5.0	96.5
4	7	2	28.6	97.7	3.0	97.5
1_4	7	3	42.9	97.3	3.9	97.2
5	7	2	28.6	98.4	4.3	98.2
6	7	1	14.3	97.9	1.7	97.7
7	7	1	14.3	97.5	1.4	97.3
8	7	6	85.7	92.4	2.8	92.4
5_8	7	7	100.0	94.6	4.5	94.6

In case of the data given in Table 4.7 which is the statistics including one neighboring site based on the theoretical binding sites, sensitivity increases to 71.4%. 10 theoretical binding sites are predicted out of 14. More binding sites are thus predicted by including the neighboring bases, which may suggest that the GNM gives a network of residues including the second shell nucleotides that may be important in antibiotics binding. 23S rRNA nucleotides 2482 (2503 E.c.) and 2432 (2453 E.c.) are not given as the known (experimental) chloramphenicol binding sites, but they are among the theoretical binding sites (Table 4.1) and they overlap with the high frequency fluctuating nucleotides given in Table 4.3. 2432 (2453 E.c.) has a functional role in the PTC region [61]. High frequency fluctuating nucleotides forming the network around the binding sites may be effective allosterically and they may be potential sites for the antibiotics resistance. For instance, nucleotide 2062 E.c. (2045 D.r.) is an important nucleotide which is not in the binding site. Its closest distance to the chloramphenicol is 7.65 Å. However, its mutation affects the binding of chloramphenicol. This nucleotide is also found by the GNM analysis as high frequency fluctuating nucleotide.

Table 4.6. Antibotics binding site prediction statistics of GNM based on the theoretical binding site data (PDB: 1K01).

Fast mode	**Bind sites count**	**TP**	**SN**	**SP**	**PRE**	**ACC**
1	**14**	**7**	**50.0**	**98.4**	**13.7**	**98.2**
2	14	1	7.1	97.8	1.6	97.3
3	14	4	28.6	98.2	7.3	97.8
4	14	2	14.3	98.7	5.4	98.3
1_4	14	3	21.4	98.5	6.8	98.1
5	14	2	14.3	99.2	8.0	98.7
6	14	2	14.3	98.9	6.1	98.4
7	14	1	7.1	98.7	2.6	98.2
8	14	6	42.9	94.7	3.9	94.4
5_8	14	6	42.9	96.9	6.5	96.6

Z-score analysis is done for all the cases and fast modes. Predicted residues' phosphate atoms are shown in Figure 4.11. Chloramphenicol is also shown in pink sticks. The high frequency fluctuating atoms in the fastest mode are colored based on the Z-scores in a range from red (lowest Z-score) to blue (highest Z-score). For this case distribution of Z-scores are given in Figure 4.11 without exact residue numbering. The mean of Z-scores of all predicted residues is -2.3 which is quite satisfactory since a Z-score below -1 is a succesful value. The minimum Z-score is -2.9 which belongs to a known binding site 2044 D.r. (2061 E.c.). The data in real residue index is given in Figure 4.13. The predicted residues which overlap with the experimentally known binding sites are shown in the figure within an ellipse. As it is expected, they have the lowest Z-scores. Their Z-scores are all lower than -2.6. All Z-scores are below -1 and the percentage of Z-scores below -2 is 44%.

Table 4.7. Antibotics binding site prediction statistics of GNM including one neighboring site based on the theoretical binding site data (PDB: 1K01).

Fast mode	**Bind sites count**	**TP**	**SN**	**SP**	**PRE**	**ACC**
1	**14**	**10**	**71.4**	**97.2**	**11.4**	**97.0**
2	14	10	71.4	96.3	9.0	96.2
3	14	10	71.4	96.7	10.0	96.6
4	14	10	71.4	98.0	15.2	97.8
1_4	14	10	71.4	97.6	13.0	97.4
5	14	10	71.4	98.7	21.3	98.5
6	14	10	71.4	98.3	17.2	98.1
7	14	10	71.4	97.9	14.5	97.7
8	14	11	78.6	92.6	5.1	92.5
5_8	14	10	71.4	94.7	6.4	94.6

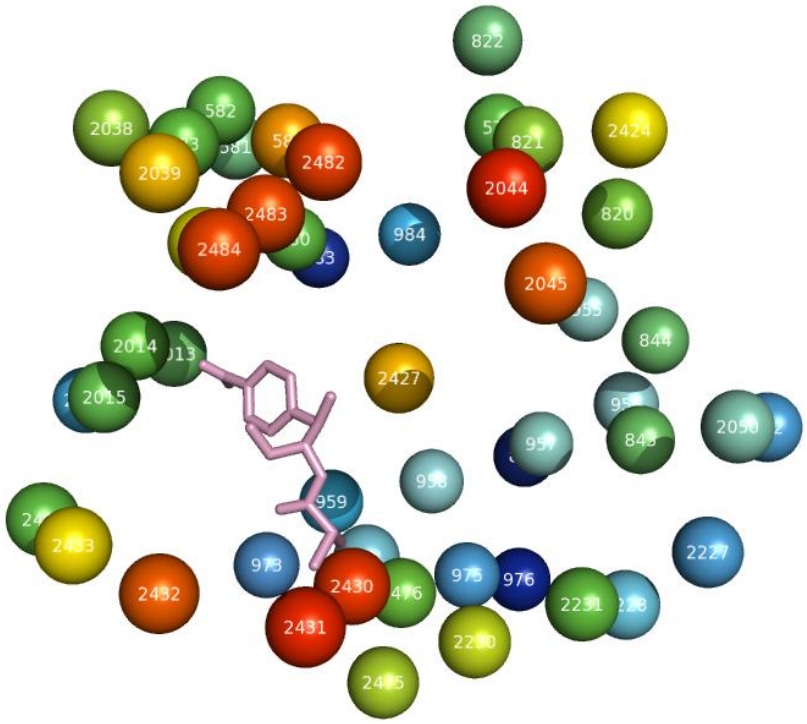

Figure 4.11. Z-scores of predicted nucleotides in space with respect to chloramphenicol (pink sticks).

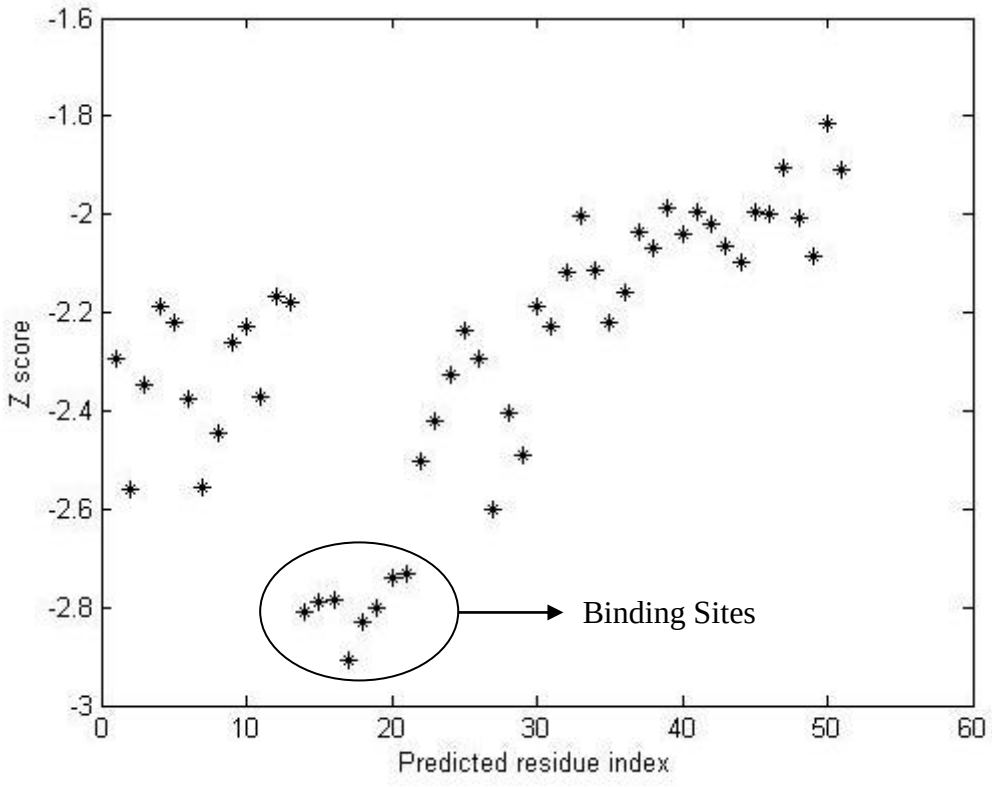

Figure 4.12. Z-scores of predicted residues (residue index is sequential).

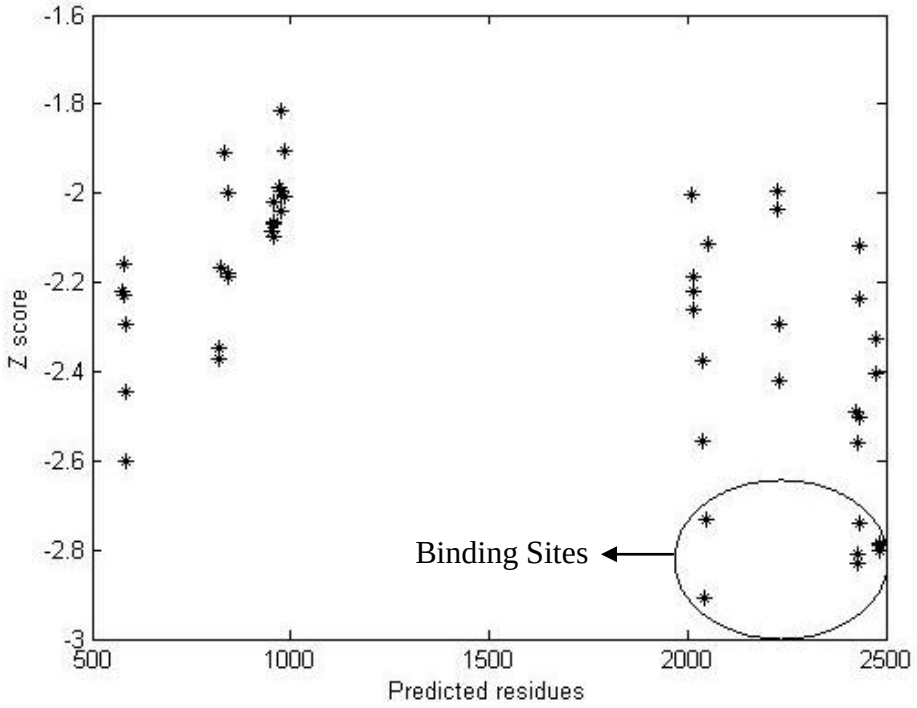

Figure 4.13. Z-scores of predicted nucleotides (residue index is real base numbering).

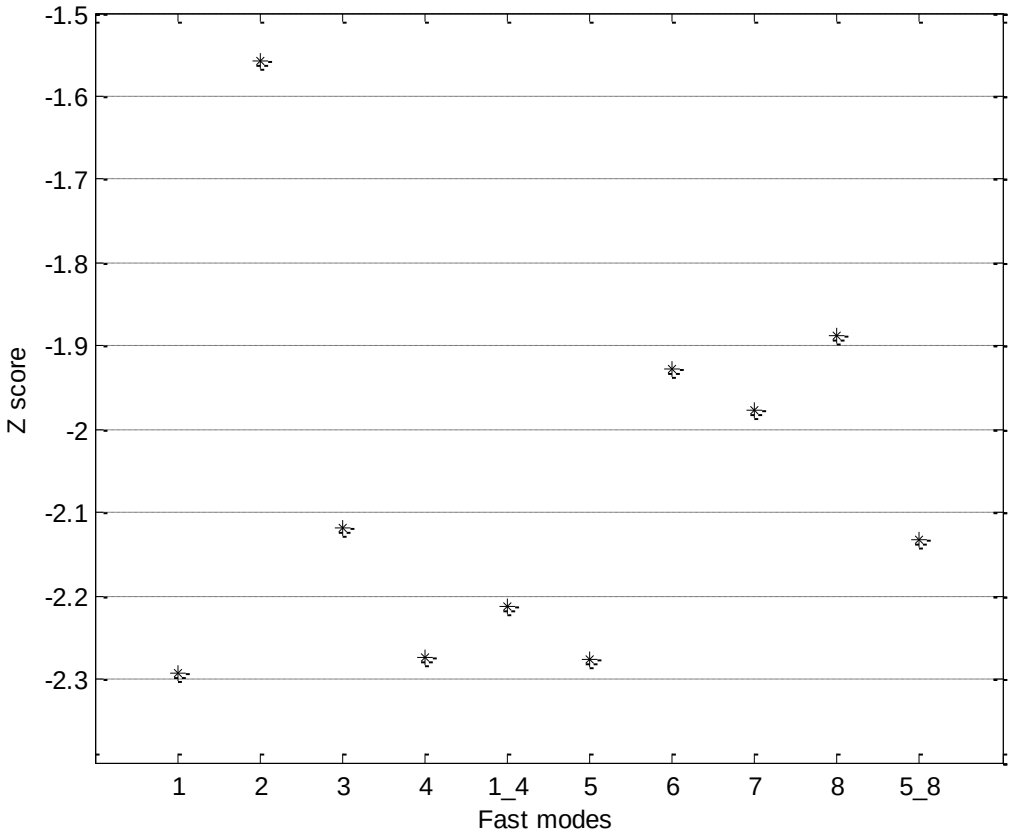

Figure 4.14. Mean Z-scores of 10 fast modes (PDB: 1K01).

Z-scores in Figure 4.11-13 belong to the predicted residues by the fastest mode. In Figure 4.14, mean Z-scores of 10 fast modes are presented. It is clear that the fastest mode has the lowest mean Z-score which means a better prediction rate.

All the data shown for this case is the data obtained by the GNM analysis with 20 Å cut-off distance. Statistics of the GNM analysis with 16 Å cut-off distance is given in the Appendix through Table A.1-4. Also, Z-score analysis of residues predicted by the fastest mode with 16 Å cut-off distance and mean Z-scores of all modes are given in Figure A.1-2. It is seen that 20 Å is a better cut-off distance.

4.5. GNM Analysis on 23S rRNA Antibiotics Unbound Ribosome Structure

The alignment of 23S ribosomal structures with antibiotics unbound structure (PDB: 1NKW) is given in Figure 4.1. GNM analysis is also done for these unbound structures. The residues having high frequency fluctuations in the fastest mode (PDB: 2ZJR) are colored according to their $\langle \Delta \mathbf{R}_{ij}^2 \rangle$ values in Figure 4.15. Aligned antibiotics structures are shown in brown sticks. It is obvious that these residues cluster in the CCA ends of tRNAs and PTC site. These sites are the most functional and antibiotics targeted sites which highly overlap with the high frequency fluctuating residues in the 50S subunit.

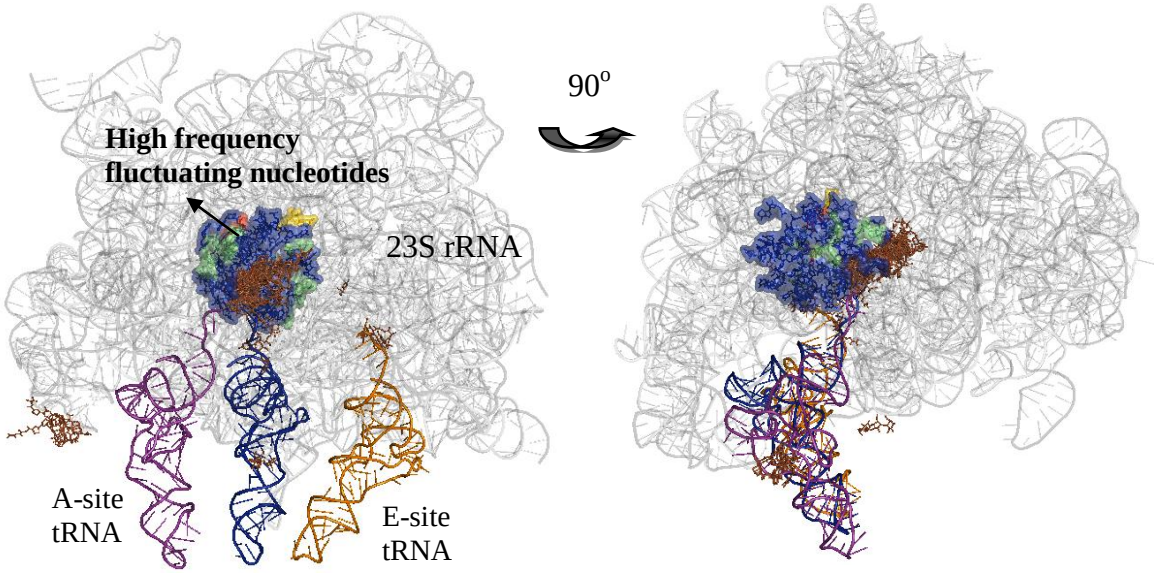

Figure 4.15. Fastest mode results for the unbound 23S rRNA (PDB: 2ZJR).

Fastest mode results for the unbound 23S rRNA and the nascent chain exit tunnel nucleotides (pink sticks with mesh representation) is given in Figure 4.16. Nucleotides shown in surface mode are the high frequency fluctuating nucleotides. The fastest mode of GNM shows that these high frequency fluctuating nucleotides are also form the walls of the nascent polypeptide chain exit tunnel entrance. The high frequency fluctuating nucleotides in the unbound structure from a network which include both the antibiotics binding sites and second shell nucleotides that do not take role in binding directly, but a mutation on that site may cause the translational inhibition. We suggest that some of these sites are potential antibiotics binding sites. Some of the high frequency fluctuating nucleotides that are in the binding sites overlap with the potential antibiotics sites revealed by deleterious mutations in *E. coli* rRNA by Mankin A. S., *et al* [62, 63].

There are 65 different theoretical binding sites in 24 *D. radiodurans* large ribosomal subunit antibiotics binding structure. 14 of these binding sites (21.5% of binding sites) are found from the fastest mode of GNM analysis (top 65 high frequency fluctuating nucleotides are selected for the fasteset mode) on unbound *D. radiodurans* structure (PDB: 2ZJR). The list of all theoretical binding sites and fastest mode high frequency fluctuating nucleotides in D. Radiodurans 23S rRNA (PDB: 2ZJR) is given in Table A.6. When one neighboring nucleotides are taken into account this number increases to 20 (30.8% of binding sites) and when two neighboring nucleotides are taken into account it even increases to 24 (36.9% of binding sites). The high frequency fluctuating nucleotides 806-807 E.c. (819-820 D.r.), 2249-2250 E.c. (2228- 2229 D.r.) and 2453 E.c. (2433 D.r.) do not overlap with the theoretical antibiotics binding sites, however they are also given by Mankin A. S., *et al*, as potential antibiotics binding sites as a result of deleterious mutation studies in *E. coli* rRNA [62]. Also, the high frequency fluctuating nucleotides 566-567 E.c. (575-576), E.c. (586 D.r.), 2029 E.c. (2012 D.r.), 2067 E.c. (2050 D.r.), 2445 E.c. (2424 D.r.), 2451 E.c. (2430 D.r.), 2454 E.c. (2433 D.r.) and 2497 E.c. (2476 D.r.) nucleotides are one or two neighboring nucleotides of the potential antibiotics binding sites given by Mankin A. S., *et al*. based on the mutational studies.

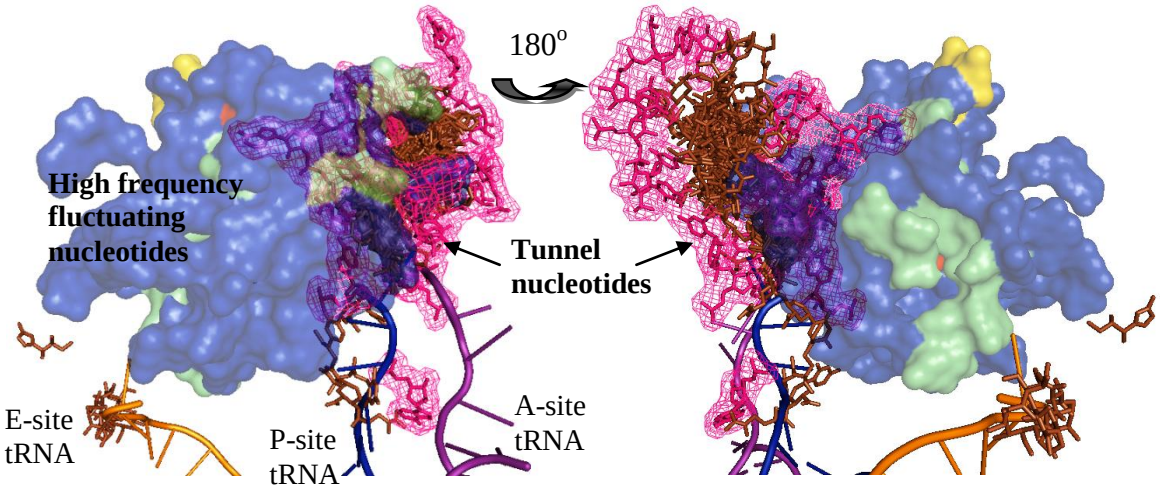

Figure 4.16. Fastest mode results for the unbound 23S rRNA and the nascent chan in exit tunnel nucleotides (PDB: 2ZJR).

It is also looked at the other fast modes. First 5 fast modes give similar results, but the sixth fast mode gives nucleotides forming the network behind the other side of the wall which is shown in Figure 4.17.

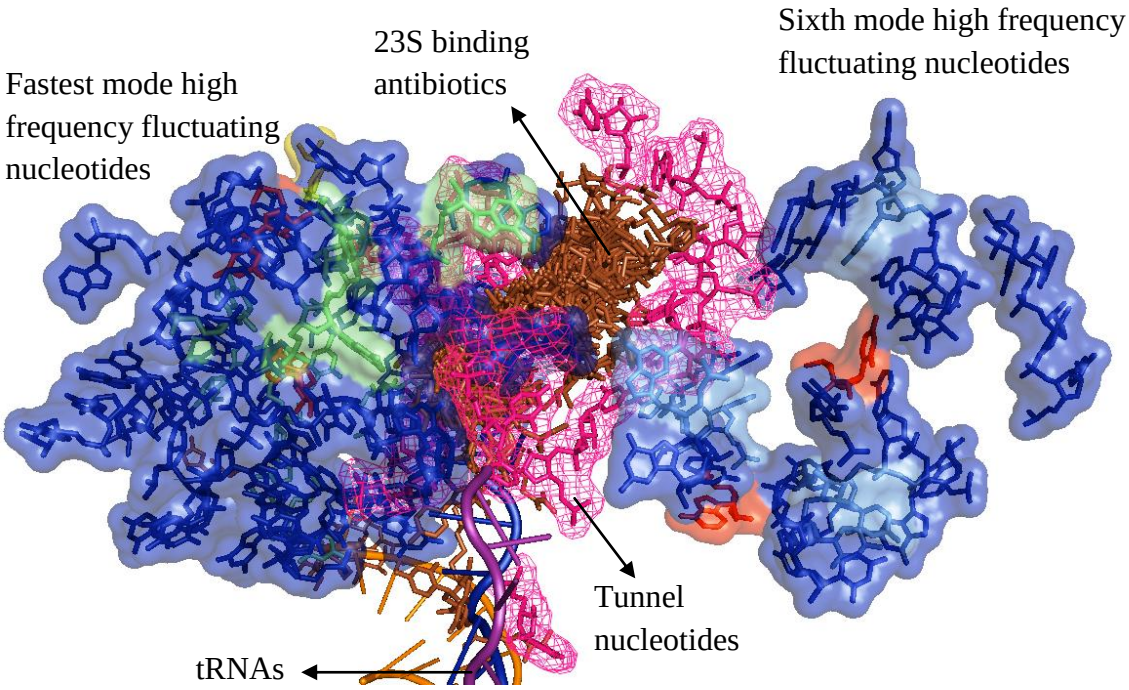

Figure 4.17. First and sixth fast mode results for the unbound 23S rRNA and the nascent chanin exit tunnel nucleotides (PDB: 2ZJR).

4.6. GNM Analysis on 16S rRNA Antibiotics Unbound Ribosome Structure

16S rRNA binding antibiotics are shown in Figure 4.18 with two different angles. These antibiotics are not clustered on the same site, but they generally bind near the anticodon region of tRNA, mRNA and the inter-subunit region. They bind only to *E.coli* and *T. thermophilus* as listed in Table 3.1. The purple and orange antibiotics in Figure 4.18-20 are *E.coli* and *T. thermophilus* binding antibiotics, respectively. The GNM analysis is carried on the antibiotics unbound *T. thermophilus* structure (PDB: 1J5E) with 20 Å cut-off distance.

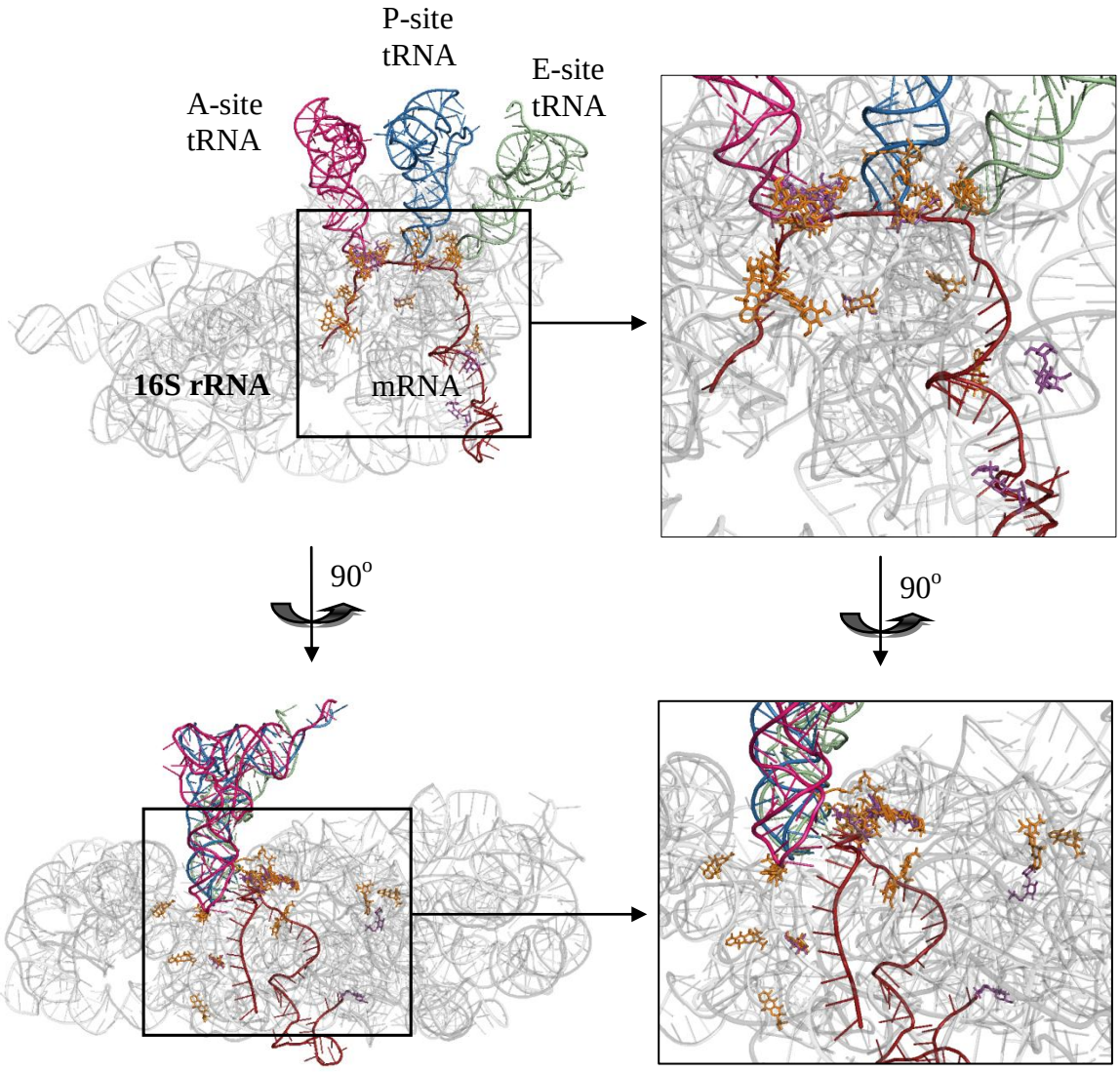

Figure 4.18. Antibotics binding on 16S rRNA.

The high frequency fluctuating nucleotides in the fastest mode are shown in blue sticks and transparent surface. They are located close to some antibiotics that bind to mRNA. They are concantrated at the core of different antibiotics binding sites (Figure 4.19). Second fast mode high frequency fluctuating nucleotides are given in Figure 4.20 which is better than the fastest mode. Just like the 23S rRNA GNM calculations slower modes like sixth mode give information about another site. In Figure 4.21, both the second and the sixth mode high frequency fluctuating nucleotides are shown. Sixth mode finds some other antibiotics binding sites such as tetracycline which binds to the A-site tRNA anticodon region. (PDB: 1HNW, 1I97). This sixth mode high frequency fluctuating nucleotides are close enough with the A and P-site tRNA to make chemical interactions. These prove that higher fast modes also located in other functionally important sites.

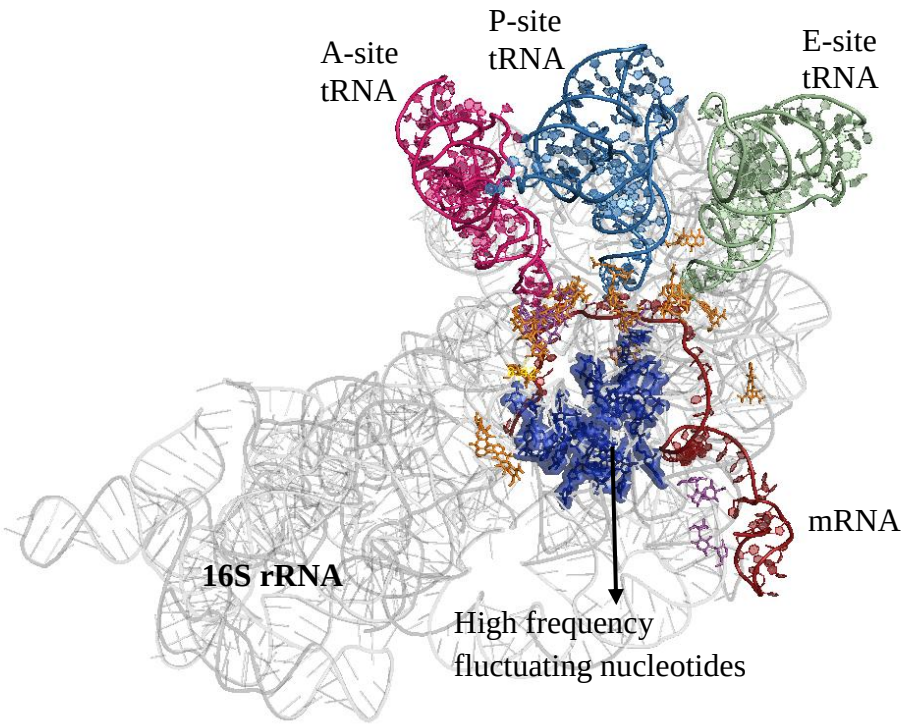

Figure 4.19. Fastest mode high frequency fluctuating nucleotides on small subunit.

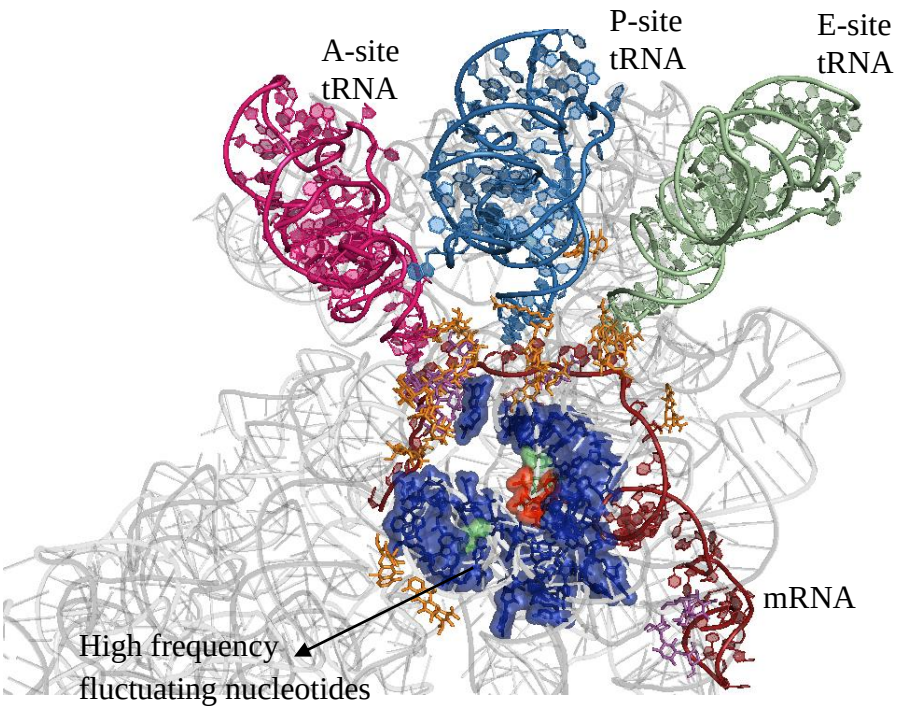

Figure 4.20. Second fast mode high frequency fluctuating nucleotides on small subunit.

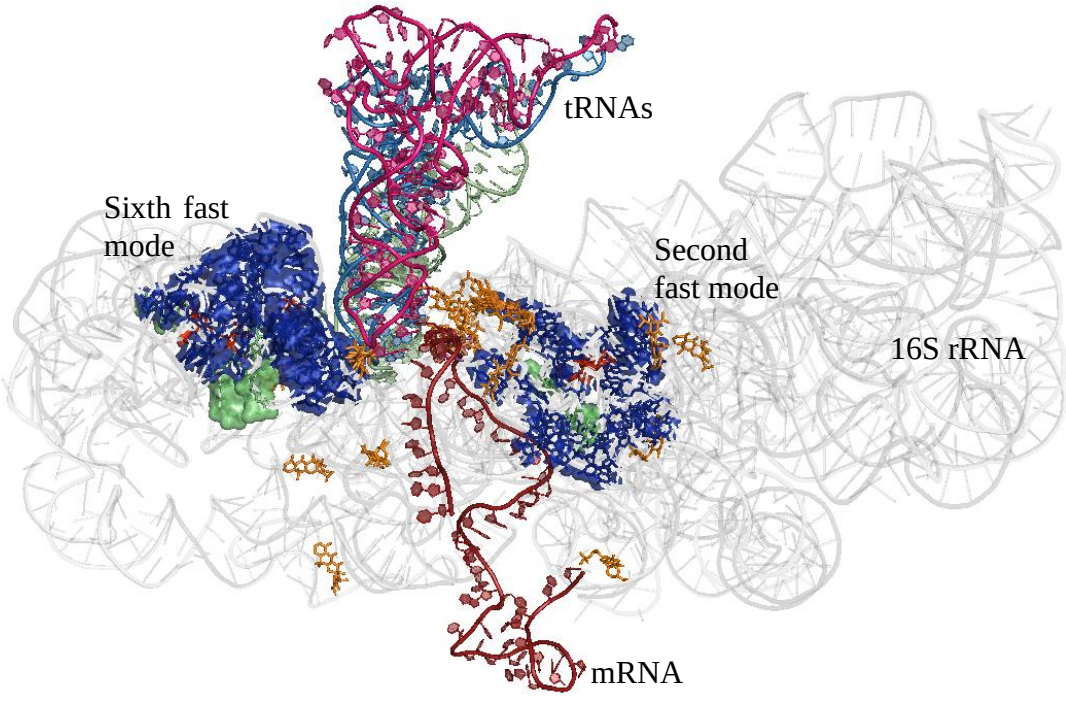

Figure 4.21. Second and sixth fast mode high frequency fluctuating nucleotides on small subunit.

4.7. GNM Analysis on 70S Ribosome Structure with 16S and 23S rRNA

GNM analysis is also done on a single structure consisting of both 16S and 23S rRNA. This is applied on 2 *E.coli* 70S structures. One of these 70S structures consists of 3DF1 (30S) and 3DF2 (50S) subunits and the other consists of 2QOY (30S) and 2QOZ (50S) subunits with approximately 4400 nodes (P atoms) for a 70S structure. Both of these structures give similar results. The analysis show that high frequency fluctuations of first 5 fast modes are in the 23S rRNA just like the GNM analysis on 23S rRNA solely. The functional sites of peptide bond synthesis are found with the fastest modes. However, high frequency fluctuations of next fast modes are concentrated in the 16S rRNA. This also proves that the functional sites in 23S rRNA are better targets for antibiotics.

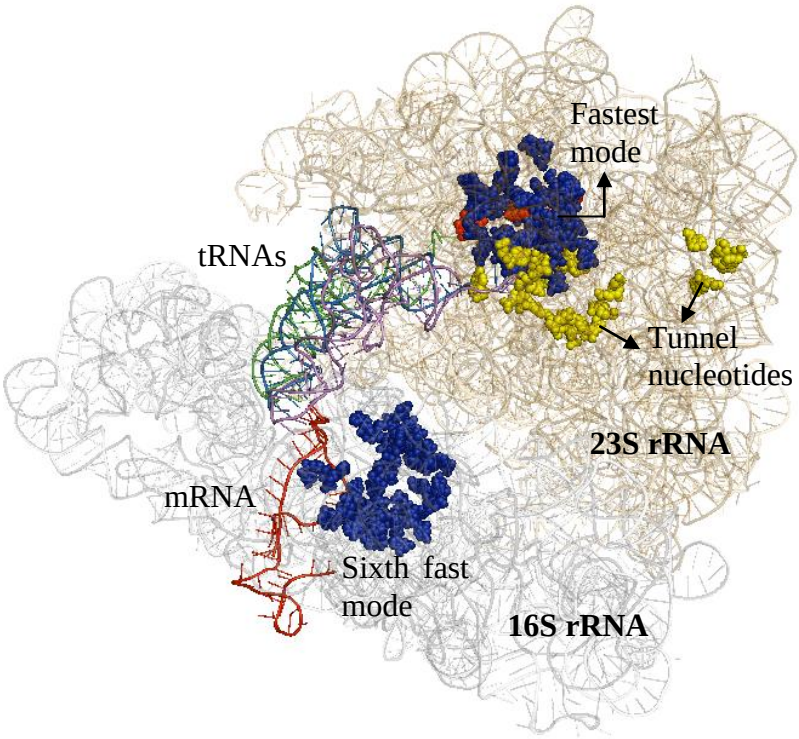

Figure 4.22. Fastest and sixth fast mode high frequency fluctuating nucleotides 70S rRNA GNM analysis.

4.8. Overall Statistics of the GNM Analysis of 64 Antibiotics Bound Structures

GNM analysis on 64 different antibiotics bound ribosome structures are subjected to obtain an overall statistics which give rise to the Table 4.8-11. When we look at the statistics of the fastest mode based on the experimental binding site data (Table 4.8), sensitivity is 19.1%. Other modes may have better results, but it is because their precision is lower than the first mode which means much more nucleotides are selected as the binding site which increases the false positives. Specificity and accuracy are almost 100%. The sensitivity increases to 28.2% when one neighboring site is included to the selected high frequency fluctuating nucleotides (Table 4.9). In case of theoretical binding sites, sensitivity is 19.8% and it is a little bit higher than the sensitivity based on the experimental binding sites, but the precision increases to 6.1% (Table 4.10). The final statistics belongs to the one neighboring site included the theoretical binding sites in which sensitivity increases to 30.5% (Table 4.11).

Table 4.8. Overall antibiotics binding site prediction statistics of GNM based on the experimental binding site data (64 antibiotics bound structures).

Fast mode	**SN**	**SP**	**PRE**	**ACC**
1	19.1	98.0	3.2	97.7
2	12.5	97.9	2.0	97.6
3	9.7	98.1	1.2	97.8
4	6.5	98.2	1.0	97.9
1_4	19.8	96.8	2.1	96.5
5	6.2	98.5	1.4	98.2
6	7.0	98.1	1.1	97.8
7	7.1	98.0	1.1	97.7
8	7.7	97.8	1.1	97.5
5_8	27.8	95.9	2.1	95.7

Table 4.9. Overall antibiotics binding site prediction statistics of GNM including one neighboring site based on the experimental binding site data (64 antibiotics bound structures).

Fast mode	SN	SP	PRE	ACC
1	28.2	96.6	2.8	96.4
2	24.4	96.8	2.4	96.5
3	17.3	97.1	1.7	96.8
4	11.7	97.3	1.2	96.9
1_4	33.0	95.9	2.7	95.6
5	11.4	97.6	1.5	97.2
6	16.1	97.1	1.6	96.8
7	15.4	97.1	1.6	96.8
8	16.4	97.0	1.7	96.7
5_8	42.7	95.3	2.9	95.1

Table 4.10. Overall antibiotics binding site prediction statistics of GNM based on the theoretical binding site data (64 antibiotics bound structures).

Fast mode	SN	SP	PRE	ACC
1	19.8	98.1	6.1	97.5
2	16.5	98.0	5.1	97.3
3	11.1	98.1	3.5	97.5
4	8.2	98.3	2.9	97.6
1_4	22.7	96.9	5.0	96.3
5	5.7	98.5	2.6	97.9
6	8.5	98.1	2.8	97.5
7	8.1	98.0	2.5	97.4
8	9.6	97.8	3.0	97.2
5_8	29.6	96.0	4.5	95.5

Table 4.11. Overall antibiotics binding site prediction statistics of GNM including one neighboring site based on the theoretical binding site data (64 antibiotics bound structures).

Fast mode	**SN**	**SP**	**PRE**	**ACC**
1	30.5	96.7	5.8	96.2
2	35.2	96.9	7.5	96.4
3	35.3	97.3	9.1	96.8
4	33.2	97.4	9.2	96.9
1_4	38.6	96.0	6.4	95.5
5	31.4	97.7	9.1	97.2
6	35.6	97.3	8.6	96.8
7	34.6	97.3	8.3	96.8
8	34.3	97.2	8.5	96.7
5_8	43.3	95.4	5.9	95.0

Mean Z-scores are calculated for all antibiotics bound structures including 10 fast modes (Figure 4.21). Antibiotics bound structure index and individual mean Z-scores are given in Figure A.5. Colormap shows the best mean Z-score value is around -2.5. Except a few cases which have positive mean Z-scores (red), almost all cases have satisfactory mean Z-scores below -1 and most below -2. It is also figured out that fastest or the other fast modes close to the fastest one gives generally better results in predicting the antibiotics binding sites.

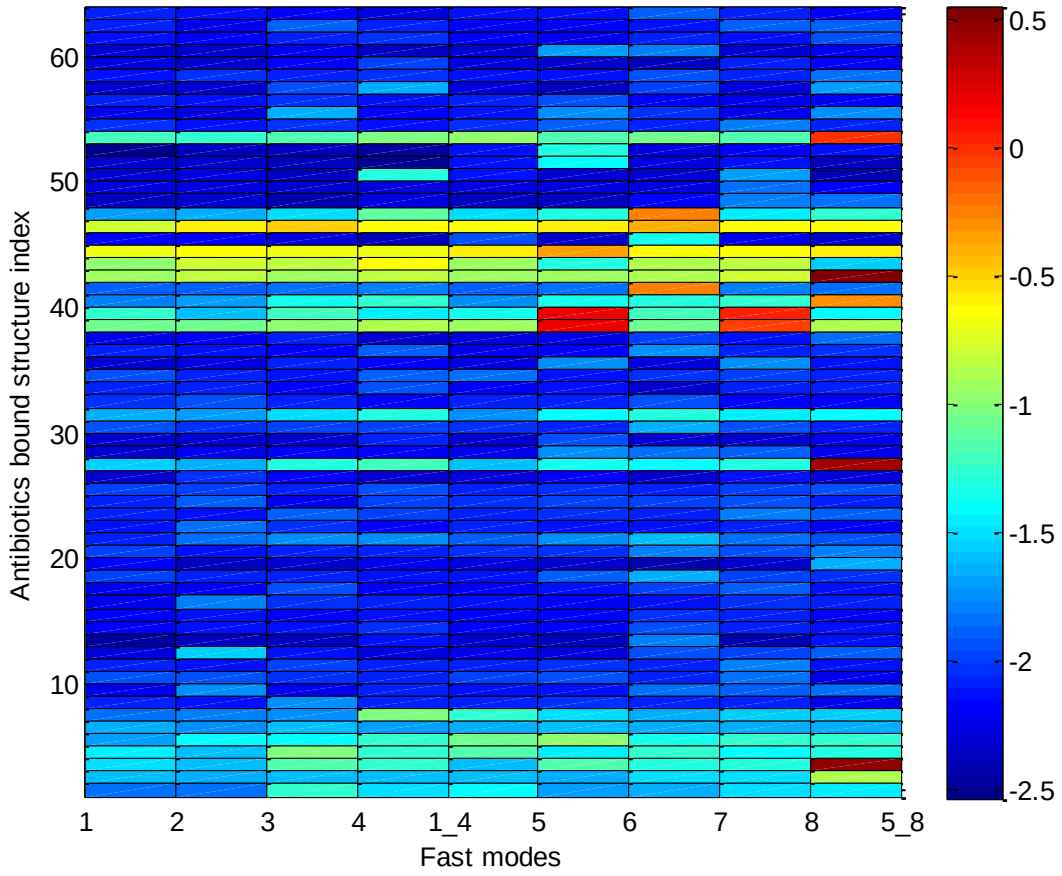

Figure 4.23. Pcolor figure of mean Z-scores of each fast mode for all structures (64 antibiotics bound structures) with 20 Å cut-off distance.

4.9. Overall Statistics of the GNM Analysis of 51 23S rRNA Antibiotics Bound Structures

51 structures out of 64 antibiotics bound structures given in Table 3.1 are 23S rRNA antibiotics binding structures. The statistics of binding site prediction is done for these 51 23S rRNA are given in Table 4.13-16. Sensitivity of fastest mode based on the known antibiotics binding sites increases to 22.8% which is 19.1% for all structure given in Table 4.8. The statistics based on the fastest mode for all structures and 23S rRNA binding structures given in Table 4.8-11 and Table 4.13-16, respectively, are summarized in Table 4.12. It is seen that the statistics based on the theoretical binding sites including one neighboring nucleotide increases to 35.2%. 24 antibiotics bound structures are *D. Radiodurans* structures among the 51 23S rRNA structures. The statistics of this group

even increases to 47.2% and 42% for the experimental and theoretical binding sites including one neighboring nucleotides. The statistics of this species is given in Table A.7-10.

Table 4.12. Overall antibiotics binding site prediction statistics of GNM based on the experimental binding site data (23S rRNA antibiotics bound structures).

		All structures				**23S rRNA binding structures**			
Binding Site	**Fast mode**	**SN**	**SP**	**PRE**	**ACC**	**SN**	**SP**	**PRE**	**ACC**
Experimental (known)	1	**19.1**	98.0	3.2	97.7	**22.8**	98.3	3.6	98.1
Experimental + one neighbor	1	**28.2**	96.6	2.8	96.4	**33.1**	97.1	3.1	97
Theoretical	1	**19.8**	98.1	6.1	97.5	**23.2**	98.4	6.9	98
Theoretical + one neighbor	1	**30.5**	96.7	5.8	96.2	**35.2**	97.2	6.5	96.9

Table 4.13. Overall antibiotics binding site prediction statistics of GNM based on the experimental binding site data (23S rRNA antibiotics bound structures).

Fast modes	**SN**	**SP**	**PRE**	**ACC**
1	22.8	98.3	3.6	98.1
2	14.9	98.2	2.3	98.0
3	12.0	98.4	1.5	98.2
4	7.9	98.4	1.1	98.2
1_4	22.8	97.4	2.3	97.2
5	7.7	98.7	1.7	98.4
6	8.4	98.2	1.2	98.0
7	8.4	98.3	1.2	98.1
8	9.2	98.1	1.3	97.9
5_8	33.4	96.4	2.4	96.3

Table 4.14. Overall antibiotics binding site prediction statistics of GNM including one neighboring site based on the experimental binding site data (23S rRNA antibiotics bound structures).

Fast modes	**SN**	**SP**	**PRE**	**ACC**
1	33.1	97.1	3.1	97.0
2	28.0	97.2	2.6	97.0
3	21.1	97.6	2.0	97.4
4	14.0	97.6	1.3	97.4
1_4	37.8	96.4	2.8	96.2
5	14.3	97.8	1.9	97.6
6	19.4	97.4	1.8	97.2
7	18.5	97.4	1.8	97.2
8	19.8	97.3	1.9	97.1
5_8	51.2	95.7	3.1	95.6

Table 4.15. Overall antibiotics binding site prediction statistics of GNM based on the theoretical binding site data (23S rRNA antibiotics bound structures).

Fast modes	SN	SP	PRE	ACC
1	23.2	98.4	6.9	98.0
2	18.6	98.2	5.7	97.8
3	13.1	98.4	4.1	98.0
4	10.1	98.5	3.4	98.0
1_4	25.8	97.5	5.7	97.1
5	7.1	98.7	3.3	98.2
6	10.6	98.3	3.5	97.8
7	9.4	98.3	2.8	97.8
8	11.5	98.1	3.5	97.7
5_8	34.8	96.5	5.1	96.2

Table 4.16. Overall antibiotics binding site prediction statistics of GNM including one neighboring site based on the theoretical binding site data (23S rRNA antibiotics bound structures).

Fast modes	SN	SP	PRE	ACC
1	35.2	97.2	6.5	96.9
2	39.9	97.3	8.2	97.0
3	40.2	97.7	10.3	97.4
4	37.8	97.8	10.0	97.5
1_4	43.8	96.5	7.0	96.2
5	36.1	98.0	9.8	97.7
6	40.5	97.6	9.5	97.3
7	39.6	97.6	9.1	97.3
8	39.8	97.5	9.6	97.2
5_8	50.0	95.8	6.5	95.6

4.10. Allosteric Interactions and Interactions with Ribosomal Proteins

As given in Section 2.3, there is a network of remote interactions between the second shell nucleotides, neighboring nucleotides and the antibiotics binding site. One example is given in chloramphenicol binding case in Section 4.4. Some of these sites are determined as the high frequency fluctuating nucleotides by GNM such as 2062 E.c. (2045 D.r.) which is not considered as a primary binding site for chloramphenicol. Likewise, second shell nucleotides for lankacidin case are 2576 (2555), 2062 (2045), 2530 (2509), 2531 (2510), 2507 (2486), 2584 (2563), 2581 (2560), 2610 (2589), and 2059 (2042). Nucleotides in parenthesis are numbered according to *D. radiodurans* structure. Among these nine second shell nucleotides, six of them are predicted by the higher fast modes. The distance between these nucleotides and lankacidin increases up to 13.5 Å in 2581 (2560) nucleotide.

The remote interactions are also exist between the antibiotics binding sites and the ribosomal proteins. Actually, antibiotics mostly bind to the rRNA, however it is reported that mutations in ribosomal proteins affects the binding when it is coupled with the mutation in rRNA. L4 is a common example to these ribosomal proteins that affect binding even though it is not close enough to the binding site to make direct interactions with the antibiotics. R111 of L4 is reported as remotely affecting the binding of antibiotics [1]. L3 and L32 are other significant ribosomal proteins which may also affect binding remotely or directly [3, 12]. Mutations on R144 and K145 (*D. radiodurans*) of L3 affects antibiotics binding remotely.

The GNM analysis on the antibiotics unbound 23S rRNA structure of *D. radiodurans* (PDB: 1NKW) show that the network of high frequency fluctuating nucleotides reach to some ribosomal proteins. Higher fast modes high frequency fluctuating nucleotides are more close the ribosomal proteins as given in Figure 4.24-25. High frequency fluctuating nucleotides are colored based on the mean square fluctuation degree as before.

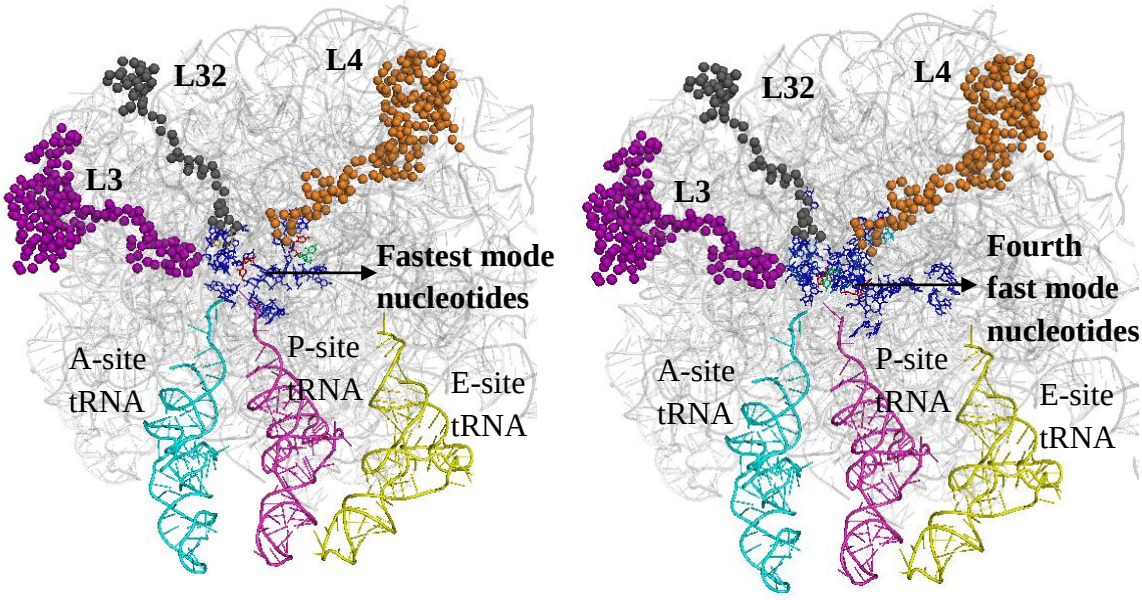

(a) (b)

Figure 4.24. Fastest (a) and fourth (b) fast mode high frequency fluctuating nucleotides near ribosomal proteins.

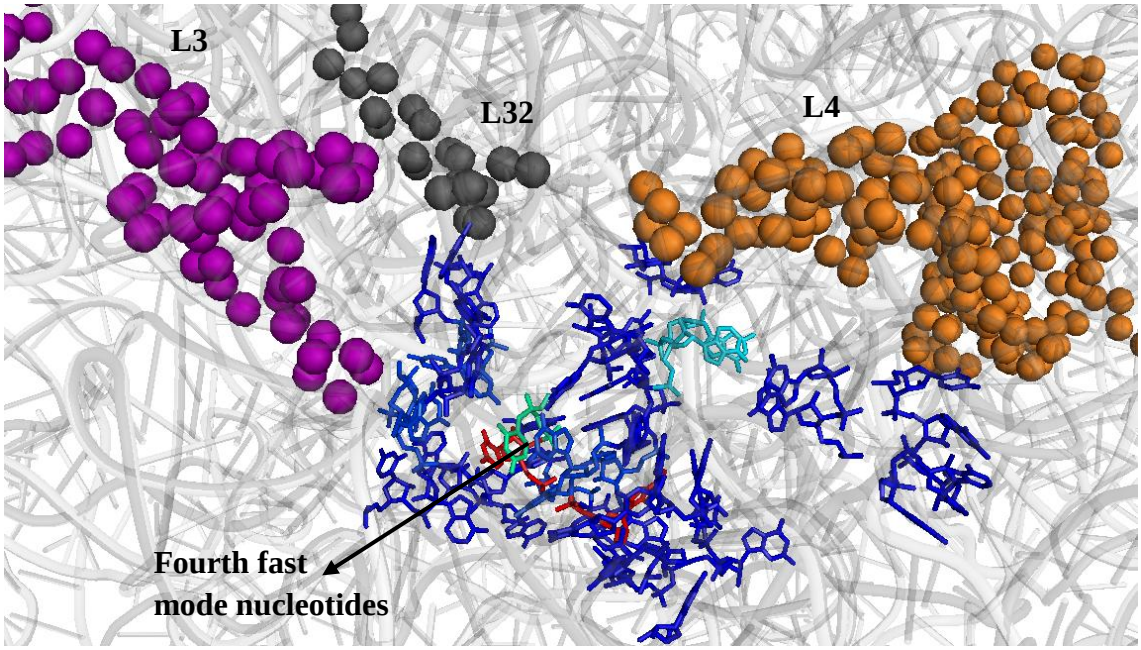

Figure 4.25. A close view of the fourth fast mode high frequency fluctuating nucleotides near ribosomal proteins.

5. CONCLUSIONS AND RECOMMENDATIONS

5.1. Conclusions

Antibiotics are widely used to control the undesired microorganism growth by various ways. Inhibition of protein synthesis in ribosome macromolecules is a common way for this control mechanism. The GNM analysis on ribosomal large subunit 23S rRNA showed that from the dynamics perspective the most plausible antibiotics target sites are the A, P, PTC sites and the entrance of the nascent polypeptide chain exit tunnel entrance which are the most functional and energetically hot sites on ribosome. On the other hand, nucleotides with high frequency fluctuations in fastest modes are in a broad region around mRNA and tRNAs. By also looking at the antibiotics bound structures, one can say that the large subunit is a better target to prevent protein synthesis. This also proved by the GNM analysis on the 70S ribosome structure including both 16S and 23S rRNA. In these calculations, the fastest modes give nucleotides with high mean distance square fluctuations at the large subunit around the PTC region. Next fast modes give high fluctuated nucleotides at the small subunit near some antibiotics binding and functional sites.

A few antibiotics bind completely to different sites than most of the other bind in the large subunit. Nucleotides of these different binding sites are not high frequency fluctuating residues, so the antibiotics binding sites could not be found. However, these sites need to be investigated one by one. For example, nosipheptide (PDB: 2ZJP) and thiostrepton (3CF5) binding sites in *D.radiodurans* are this kind of binding sites with no high frequency fluctuating residue. The reason for this might be due the fact that they do not bind ribosome with high affinity without the ribosomal protein L11 [41].

Sensitivity of finding the antibiotics binding site increases up to 100% when including 1 neighboring residues in some cases. The sensitivity based on the theoretical antibiotics binding sites of the GNM analysis with 20 Å cut-off distance on the 64 antibiotics bound structures is 19.8% and this increases to 30.5% when one neighboring

nucleotides are included. In 51 large ribosomal subunits, sensitivity even increases to 35.2%.

The GNM analysis on the antibiotics unbound ribosomal structures revealed that the antibiotics binding sites can be predicted with unbound ribosomal structures. Besides the accurately predicted antibiotics binding sites, the second shell nucleotides are also predicted which affect binding upon mutation. Some of the predicted sites which are not theoretical binding sites are potential binding sites which overlap with the potential binding sites reported by Mankin A. S., *et al* [62, 63]. The higher fast modes are significant in these second shell nucleotides and nucleotides that are close to the ribosomal proteins.

5.2. Recommendations

This thesis is dedicated to find the antibiotics binding sites of a dataset given in Table 3.1. GNM analysis is done on every structure and statistics are extracted for the high mean square fluctuations. After this level, data for each structure will be studied separately since ribosome is a very complex macromolecule and there are lots of interactions associated with mRNA, tRNA, rRNA, ribosomal proteins and other factors. Antibiotics mostly bind to the rRNA, however, GNM analysis on the ribosome structure including both rRNA and ribosomal proteins may be carried out to better figure out the rest of the possible antibiotics binding sites, especially the ones that are also in interaction with ribosomal proteins with high affinity compared to rRNA.

APPENDIX A: GNM STATISTICS

Table A.1. Antibotics binding site prediction statistics of GNM based on the experimental binding site data (PDB: 1K01) with cut-off 16 Å.

Fast mode	Bind sites count	TP	SN	SP	PRE	ACC
1	7	3	42.9	97.4	4.1	97.3
2	7	0	0.0	98.1	0.0	97.9
3	7	1	14.3	99.1	4.0	98.9
4	7	0	0.0	97.1	0.0	96.9
1_4	7	1	14.3	97.4	1.4	97.2
5	7	0	0.0	99.0	0.0	98.7
6	7	2	28.6	98.5	4.7	98.3
7	7	0	0.0	98.2	0.0	98.0
8	7	2	28.6	97.7	3.1	97.5
5_8	7	1	14.3	96.6	1.1	96.4

Table A.2. Antibotics binding site prediction statistics of GNM including one neighboring site based on the experimental binding site data (PDB: 1K01) with cut-off 16 Å.

Fast mode	Bind sites count	TP	SN	SP	PRE	ACC
1	7	6	85.7	95.4	4.5	95.4
2	7	0	0.0	96.5	0.0	96.3
3	7	1	14.3	98.1	1.9	97.9
4	7	0	0.0	94.7	0.0	94.4
1_4	7	1	14.3	95.3	0.8	95.1
5	7	0	0.0	97.8	0.0	97.6
6	7	5	71.4	97.3	6.2	97.2
7	7	0	0.0	96.7	0.0	96.5
8	7	5	71.4	95.8	4.2	95.8
5_8	7	2	28.6	93.6	1.1	93.5

Table A.3. Antibotics binding site prediction statistics of GNM based on the theoretical binding site data (PDB: 1K01) with cut-off 16 Å.

Fast mode	**Bind sites count**	**TP**	**SN**	**SP**	**PRE**	**ACC**
1	14	4	28.6	97.5	5.4	97.1
2	14	0	0.0	98.1	0.0	97.6
3	14	2	14.3	99.2	8.0	98.7
4	14	1	7.1	97.1	1.3	96.7
1_4	14	2	14.3	97.4	2.7	97.0
5	14	0	0.0	98.9	0.0	98.4
6	14	3	21.4	98.6	7.0	98.2
7	14	1	7.1	98.3	2.0	97.8
8	14	3	21.4	97.8	4.6	97.4
5_8	14	4	28.6	96.7	4.2	96.4

Table A.4. Antibotics binding site prediction statistics of GNM including one neighboring site based on the theoretical binding site data (PDB: 1K01) with cut-off 16 Å.

Fast mode	**Bind sites count**	**TP**	**SN**	**SP**	**PRE**	**ACC**
1	14	8	57.1	95.5	6.0	95.3
2	14	8	57.1	96.8	8.3	96.6
3	14	1	7.1	98.1	1.9	97.6
4	14	8	57.1	95.0	5.4	94.8
1_4	14	8	57.1	95.5	6.1	95.3
5	14	4	28.6	98.0	6.7	97.6
6	14	8	57.1	97.4	9.9	97.2
7	14	8	57.1	97.0	8.8	96.8
8	14	8	57.1	95.9	6.7	95.7
5_8	14	9	64.3	93.9	5.1	93.7

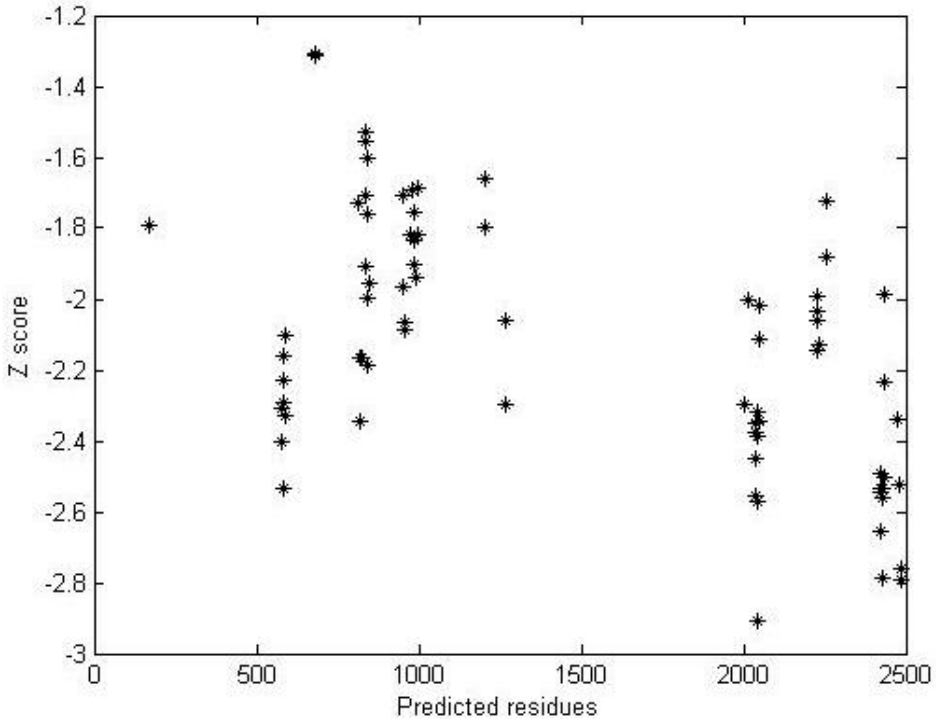

Figure A.1. Z-scores of predicted nucleotides (residue index is real base numbering) with cut-off 16 Å.

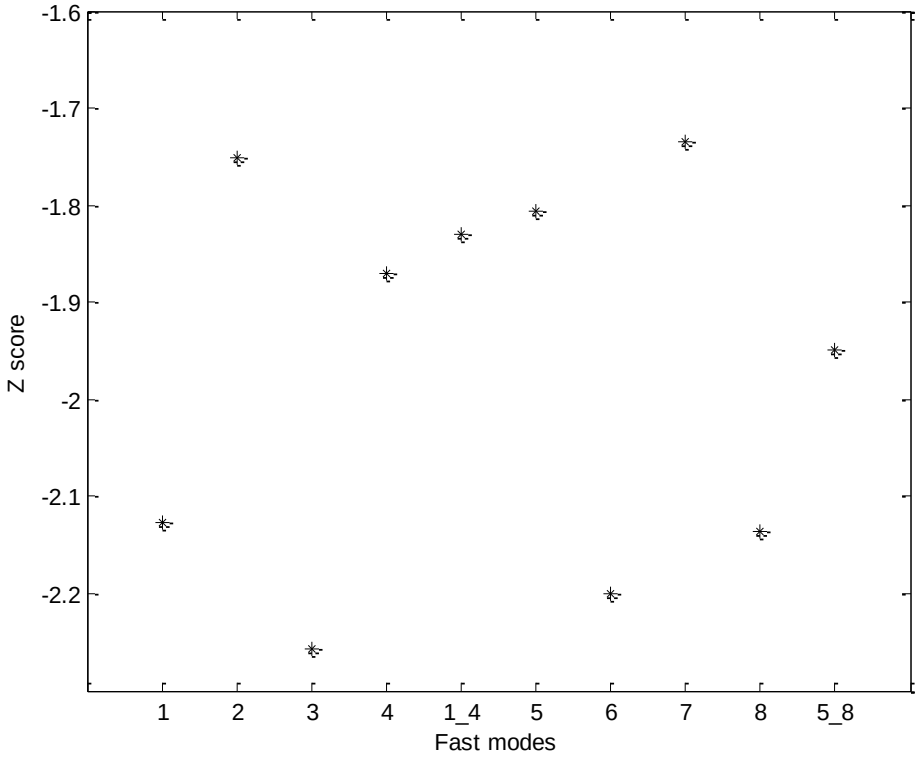

Figure A.2. Mean Z-scores of 10 fast modes (PDB: 1K01) with cut-off 16 Å.

Table A.5. Mean Z-score values of fast modes of all structures.

Structure index	PDB ID	Fast mode									
		1	2	3	4	1_4	5	6	7	8	5_8
1	1FJG	-1.83	-1.82	-1.28	-1.49	-1.40	-1.68	-1.66	-1.51	-1.44	-1.39
2	1HNW	-1.62	-1.66	-1.59	-1.62	-1.60	-1.65	-1.50	-1.51	-0.89	-1.55
3	1HNX	-1.49	-1.58	-1.18	-1.24	-1.59	-1.17	-1.33	-1.30	0.48	-1.14
4	1HNZ	-1.44	-1.62	-1.02	-1.28	-1.16	-1.45	-1.26	-1.42	-1.33	-1.13
5	1I95	-1.68	-1.42	-1.41	-1.26	-1.06	-0.97	-1.34	-1.27	-1.27	-1.16
6	1I97	-1.63	-1.72	-1.60	-1.68	-1.65	-1.59	-1.63	-1.65	-1.66	-1.71
7	1IBK	-1.82	-1.79	-1.74	-1.02	-1.25	-1.49	-1.63	-1.56	-1.56	-1.23
8	1J5A	-2.09	-2.11	-1.74	-2.09	-2.07	-2.03	-2.08	-2.06	-2.23	-2.03
9	1JZX	-2.22	-1.77	-2.21	-2.10	-2.14	-2.13	-1.81	-1.89	-1.85	-1.94
10	1JZY	-1.93	-1.95	-2.05	-2.08	-2.00	-1.95	-2.09	-1.83	-2.20	-2.07
11	1JZZ	-2.08	-2.14	-1.99	-2.08	-2.09	-2.01	-2.06	-1.79	-2.14	-2.10
12	1K01	-2.29	-1.56	-2.12	-2.27	-2.21	-2.28	-1.93	-1.98	-1.89	-2.13
13	1K73	-2.46	-2.36	-2.38	-2.15	-2.33	-2.36	-1.77	-2.40	-2.12	-2.24
14	1K8A	-2.19	-2.15	-2.12	-2.05	-2.16	-2.19	-1.94	-2.07	-2.14	-2.20
15	1K9M	-2.19	-2.13	-2.18	-2.14	-2.20	-2.17	-2.05	-2.06	-2.19	-2.15
16	1KC8	-2.25	-1.78	-2.04	-2.08	-2.15	-2.18	-2.11	-2.04	-2.06	-2.09
17	1KD1	-2.24	-2.17	-1.94	-2.17	-2.16	-2.12	-1.99	-1.87	-2.12	-2.13
18	1M1K	-1.99	-2.08	-2.10	-2.13	-2.11	-1.87	-1.65	-1.96	-2.05	-2.05
19	1N8R	-2.16	-2.35	-2.34	-2.22	-2.29	-2.33	-2.43	-2.34	-1.66	-2.23
20	1NJI	-1.98	-2.14	-2.10	-2.08	-2.04	-2.02	-1.80	-1.92	-1.79	-2.01
21	1NJN	-2.08	-1.85	-1.72	-1.73	-1.88	-1.73	-1.61	-1.85	-1.92	-1.85
22	1NWX	-2.12	-1.82	-2.01	-2.15	-2.07	-2.12	-2.12	-2.10	-2.19	-2.08
23	1NWY	-2.06	-2.12	-1.87	-2.00	-2.09	-2.05	-2.07	-1.81	-1.90	-2.08
24	1OND	-2.08	-1.91	-2.24	-2.00	-2.04	-1.97	-2.00	-1.95	-2.08	-2.06
25	1P9X	-2.00	-1.98	-2.10	-1.95	-2.07	-2.06	-2.06	-1.97	-1.95	-2.02
26	1SM1	-2.33	-2.05	-2.17	-2.31	-2.28	-2.19	-2.31	-2.12	-2.26	-2.21
27	1VS5	-1.56	-1.66	-1.31	-1.23	-1.58	-1.36	-1.43	-1.32	0.41	-1.23
28	1XBP	-2.33	-2.22	-2.19	-2.16	-2.23	-1.72	-1.86	-1.88	-2.21	-2.14
29	1YIT	-2.34	-2.34	-2.34	-2.07	-2.32	-1.94	-2.34	-2.34	-2.22	-2.27
30	1Z58	-1.92	-2.05	-1.98	-1.97	-2.02	-2.08	-1.62	-1.93	-2.07	-2.02
31	2HHH	-1.64	-1.69	-1.50	-1.32	-1.73	-1.40	-1.32	-1.45	-1.42	-1.33
32	2O43	-2.04	-1.94	-2.10	-2.17	-2.08	-2.08	-1.93	-2.16	-2.17	-2.04
33	2O44	-2.10	-2.07	-2.15	-1.96	-2.20	-2.11	-2.31	-2.09	-2.08	-2.13

Table A.5. Mean Z-score values of fast modes of all structures, cont.

Structure index	PDB ID	Fast mode									
		1	2	3	4	1_4	5	6	7	8	5_8
34	**2O45**	-1.94	-2.08	-2.12	-1.89	-1.85	-2.13	-2.02	-1.97	-2.09	-1.95
35	**2OGM**	-2.32	-2.28	-2.10	-2.17	-2.28	-1.72	-2.26	-1.73	-2.15	-2.19
36	**2OGN**	-2.08	-2.14	-2.17	-1.89	-2.22	-2.18	-1.76	-2.09	-2.02	-2.17
37	**2OGO**	-2.25	-2.19	-2.06	-2.32	-2.28	-2.20	-1.97	-2.14	-1.83	-2.18
38	**2OTJ**	-1.05	-1.06	-0.98	-0.85	-0.94	0.20	-1.08	-0.07	-0.86	-0.78
39	**2OTL**	-1.28	-1.59	-1.21	-1.46	-1.38	0.21	-1.20	0.03	-1.43	-1.32
40	**2QAL**	-1.79	-1.71	-1.34	-1.25	-1.73	-1.35	-1.33	-1.28	-0.27	-1.37
41	**2QB9**	-1.89	-1.87	-1.84	-1.81	-1.86	-1.84	-0.26	-1.78	-1.83	-1.61
42	**2QOU**	-0.94	-0.80	-0.92	-0.82	-0.92	-0.90	-0.89	-0.77	0.55	-0.52
43	**2QOZ**	-0.96	-0.78	-0.84	-0.63	-0.93	-1.32	-0.88	-0.83	-1.54	-0.99
44	**2ZJP**	-0.66	-0.61	-0.67	-0.66	-0.60	-0.32	-0.63	-0.61	-0.59	-0.59
45	**3CC4**	-2.20	-2.19	-2.26	-2.35	-1.95	-2.33	-1.38	-2.22	-2.33	-2.18
46	**3CF5**	-0.77	-0.60	-0.49	-0.65	-0.65	-0.58	-0.38	-0.63	-0.63	-0.66
47	**3DF1**	-1.69	-1.65	-1.50	-1.13	-1.50	-1.31	-0.27	-1.47	-1.26	-1.24
48	**3DLL**	-2.35	-2.34	-2.40	-2.28	-2.37	-2.35	-2.17	-1.80	-1.86	-2.28
49	**3FWO**	-2.27	-2.29	-2.30	-2.26	-2.26	-2.26	-2.26	-1.84	-2.20	-2.22
50	**3G4S**	-2.32	-2.28	-2.37	-1.32	-2.13	-2.30	-2.32	-1.67	-2.39	-2.15
51	**3G6E**	-2.30	-2.33	-2.39	-2.54	-2.13	-1.39	-2.29	-2.12	-2.36	-2.21
52	**3G71**	-2.51	-2.38	-2.37	-2.48	-2.14	-1.31	-2.29	-2.18	-2.15	-2.32
53	**3I55**	-1.19	-1.26	-1.14	-1.03	-0.98	-1.15	-1.09	-1.18	-0.01	-0.99
54	**3I56**	-2.03	-2.14	-2.03	-2.15	-2.05	-1.88	-2.09	-1.79	-2.09	-2.08
55	**3JQ4**	-2.23	-2.26	-1.65	-2.20	-2.13	-1.73	-2.01	-2.22	-1.72	-2.11
56	**3OAT**	-2.08	-2.14	-2.03	-2.15	-2.09	-1.91	-2.15	-2.21	-2.16	-2.09
57	**3OFC**	-2.33	-2.34	-1.94	-1.64	-2.28	-2.39	-2.00	-2.27	-1.71	-2.26
58	**3OFR**	-2.14	-2.04	-2.07	-2.01	-2.11	-2.10	-1.95	-2.08	-1.83	-2.08
59	**3OFZ**	-2.27	-2.30	-2.16	-1.96	-2.28	-2.31	-2.39	-2.08	-2.17	-2.21
60	**3OH5**	-2.34	-2.33	-2.20	-2.35	-2.31	-1.69	-1.80	-2.31	-2.23	-2.24
61	**3OHJ**	-2.11	-2.18	-2.10	-2.02	-2.15	-2.23	-2.10	-2.13	-1.91	-2.11
62	**3OI1**	-2.09	-2.22	-1.87	-2.08	-2.18	-2.20	-2.12	-1.88	-1.87	-2.11
63	**3OI3**	-2.10	-2.11	-2.16	-2.27	-2.14	-2.11	-1.89	-2.09	-2.19	-2.09
64	**3ORB**	-2.10	-2.12	-1.89	-2.11	-2.10	-1.88	-2.11	-2.16	-1.94	-2.08

Table A.6. All theoretical binding sites and fastest mode high frequency fluctuating nucleotides in D. Radiodurans 23S rRNA (PDB: 2ZJR).

Theoretical binding sites in D. Radiodurans 23S rRNA	Theoretical binding sites in D. Radiodurans 23S rRNA	Fastest mode high frequency fluctuating nucleotides	Fastest mode high frequency fluctuating nucleotides
758	2416	575	2015
759	2417	576	2016
760	2418	578	2038
761	2419	579	2039
764	2420	580	2040
765	2421	581	2044
798	2422	582	2045
802	2426	583	2046
803	2430	584	2047
804	2431	585	2048
805	2432	586	2049
1078	2479	819	2050
1079	2482	820	2227
1080	2483	821	2228
1081	2484	822	2229
1106	2485	835	2230
1107	2486	842	2231
1771	2551	843	2424
1772	2552	844	2427
1773	2555	955	2430
1774	2560	956	2431
2039	2562	957	2432
2040	2563	958	2433
2041	2564	959	2434
2042	2565	960	2435
2044	2566	972	2474
2045	2580	973	2475
2046	2581	974	2476
2047	2587	975	2481
2048	2588	984	2482
2231	2589	2012	2483
2232	2590	2013	2484
2233		2014	

Table A.7. Overall antibiotics binding site prediction statistics of GNM based on the experimental binding site data (*D. radiodurans* antibiotics bound structures).

Fast mode	SN	SP	PRE	ACC
1	31.8	98.3	5.0	98.1
2	17.5	98.0	2.4	97.7
3	12.0	98.6	1.6	98.3
4	5.7	98.7	1.0	98.4
1_4	33.1	97.4	3.4	97.2
5	9.0	98.8	2.1	98.5
6	9.4	98.4	1.9	98.2
7	10.0	98.1	1.5	97.8
8	14.1	97.7	1.9	97.4
5_8	41.8	96.4	3.1	96.2

Table A.8. Overall antibiotics binding site prediction statistics of GNM including one neighboring site based on the experimental binding site data (*D. radiodurans* antibiotics bound structures).

Fast mode	SN	SP	PRE	ACC
1	47.2	97.1	4.4	96.9
2	31.1	96.8	2.7	96.6
3	21.2	97.6	2.1	97.4
4	10.8	97.8	1.2	97.6
1_4	50.3	96.2	3.8	96.0
5	16.7	97.8	2.2	97.6
6	20.0	97.6	2.3	97.4
7	23.3	97.1	2.3	96.9
8	29.6	97.0	2.8	96.8
5_8	58.7	95.4	3.6	95.3

Table A.9. Overall antibiotics binding site prediction statistics of GNM based on the theoretical binding site data (*D. radiodurans* antibiotics bound structures).

Fast mode	**SN**	**SP**	**PRE**	**ACC**
1	27.2	98.4	8.1	98.0
2	16.1	98.0	4.4	97.6
3	10.2	98.6	3.8	98.1
4	5.4	98.7	2.1	98.2
1_4	27.5	97.5	5.9	97.1
5	6.5	98.8	3.4	98.3
6	10.2	98.5	3.8	98.0
7	8.5	98.1	2.4	97.6
8	12.6	97.7	3.6	97.2
5_8	33.3	96.4	4.8	96.1

Table A.10. Overall antibiotics binding site prediction statistics of GNM including one neighboring site based on the theoretical binding site data (*D. radiodurans* antibiotics bound structures).

Fast mode	**SN**	**SP**	**PRE**	**ACC**
1	42.0	97.2	7.7	96.9
2	44.5	97.0	9.0	96.7
3	42.2	97.8	11.3	97.5
4	40.4	98.0	11.7	97.7
1_4	50.0	96.3	7.6	96.1
5	43.2	98.0	12.4	97.7
6	41.9	97.8	11.0	97.5
7	46.1	97.3	10.2	97.0
8	45.0	97.1	10.2	96.8
5_8	54.3	95.5	6.9	95.3

REFERENCES

1. Schlunzen, F., R. Zarivach, J. Harms, A. Bashan, A. Tocilj, R. Albrecht, A. Yonath, F. Franceschi, "Structural basis for the interaction of antibiotics with the peptidyl transferase centre in eubacteria", *Nature*, Vol. 413, No. 6858, pp. 814-821, 2001.

2. Schlunzen, F., J. M Harms, F. Franceschi, H. A. Hansen, H. Bartels, R. Zarivach, A. Yonath, "Structural basis for the antibiotic activity of ketolides and azalides", *Structure*, Vol. 11, No. 3, pp. 329-338, 2003.

3. Berisio, R., F. Schluenzen, J. Harms, A. Bashan, T. Auerbach, D. Baram, A. Yonath, "Structural insight into the role of the ribosomal tunnel in cellular regulation", *Nature Structural Biology*, Vol. 10, No. 5, pp. 366-370, 2003.

4. Pyetan, E., D. Baram, T. Auerbach-Nevo, A. Yonath, "Chemical parameters influencing fine tuning in the binding of macrolide antibiotics to the ribosomal tunnel", *Pure and Applied Chemistry*, Vol. 79, No. 6, pp. 955-968, 2007.

5. Auerbach, T., I. Mermershtain, A. Bashan, C. Davidovich, C. H. Rozenberg, D. H. Sherman, A. Yonath, "Structural basis for the antibacterial activity of the 12-membered-ring mono-sugar macrolide methymycin", *Biotechnologia*, Vol. 1, No. 84, pp. 24-35, 2009.

6. Dunkle, J. A., L. Xiong, A. S. Mankin, J. H. Cate, "Structures of the Escherichia coli ribosome with antibiotics bound near the peptidyl transferase center explain spectra of drug action", *Proceedings of the National Academy of Sciences of the United States of America*, Vol. 107, No. 40, pp. 17152-17157, 2010.

7. Hansen, J. L., J. A. Ippolito, N. Ban, P. Nissen, P. B. Moore, T. A. Steitz, "The structures of four macrolide antibiotics bound to the large ribosomal subunit", *Molecular Cell.*, Vol. 10, No. 1, pp. 117-128, 2002.

8. Berisio, R., J. Harms, F. Schluenzen, R. Zarivach, H.A. Hansen, P. Fucini, A. Yonath, "Structural insight into the antibiotic action of telithromycin against resistant mutants", *Journal of Bacteriology*, Vol. 185, No. 14, pp. 4276-4279, 2003.

9. Llano-Sotelo, B., J. Dunkle, D. Klepacki, W. Zhang, P. Fernandes, J. H. Cate, A. S. Mankin, "Binding and action of CEM-101, a new fluoroketolide antibiotic that inhibits protein synthesis", *Antimicrobial Agents Chemotherapy*, Vol. 54, No. 12, pp. 4961-4970, 2010.

10. Wilson, D.N., F. Schluenzen, J. M. Harms, A. L. Starosta, S. R. Connell, P. Fucini, "The oxazolidinone antibiotics perturb the ribosomal peptidyl-transferase center and effect tRNA positioning", *Proceedings of the National Academy of Sciences of the United States of America*, Vol. 105, No. 36, pp. 13339-13344, 2008.

11. Gregory, S. T., A. E. Dahlberg, "Erythromycin resistance mutations in ribosomal proteins L22 and L4 perturb the high order structure of 23S ribosomal RNA", *Journal of Molecular Biology*, Vol. 289, No. 4, pp. 827-834, 1999.

12. Schluenzen, F., E. Pyetan, P. Fucini, A. Yonath, J. M. Harms, "Inhibition of peptide bond formation by pleuromutilins: the structure of the 50S ribosomal subunit from Deinococcus radiodurans in complex with tiamulin", *Molecular Microbiology*, Vol. 54, No. 5, pp. 1287-1294, 2004.

13. Harms, J. M., F. Schlunzen, P. Fucini, H. Bartels, A. Yonath, "Alterations at the peptidyl transferase centre of the ribosome induced by the synergistic action of the streptogramins dalfopristin and quinupristin", *BMC Biology*, Vol. 2, No. 4, p. 4, 2004.

14. Bashan, A., I. Agmon, R. Zarivatch, F. Schluenzen, J. M. Harms, R. Berisio, H. Bartels, F. Franceschi, T. Auerbach, H. A. Hansen, E. Kossoy, M. Kessler, A. Yonath, "Structural Basis of the Ribosomal Machinery for Peptide Bond Formation, Translocation, and Nascent Chain Progression", *Molecular Cell*, Vol. 11, No. 1, pp. 91-102, 2003.

15. David-Eden, H., A.S. Mankin, Y. Mandel-Gutfreund, "Structural signatures of antibiotic binding sites on the ribosome", *Nucleic Acids Research*, Vol. 38, No. 18, pp. 1-13, 2010.

16. Mathews, C. K., K. E. van Holde, K. G. Ahern, *Biochemistry*, 3rd Edition, Addison Wesley Longman Inc., San Francisco, 2000.

17. Borovinskaya, M. A., R. D. Pai, W. Zhang, B. S. Schuwirth, J. M. Holton, G. Hirokawa, H. Kaji, A. Kaji, J. H. Cate, "Structural basis for aminoglycoside inhibition of bacterial ribosome recycling", *Nature Structural & Molecular Biology*, Vol. 14, No. 8, pp. 727-732, 2007.

18. Wilson, D. N. "The A-Z of bacterial translation inhibitors", *Critical Reviews in Biochemistry and Molecular Biology,* Vol. 44, No. 6, pp. 393-433, 2009.

19. Nissen, P., S. Thirup, M. Kjeldgaard, J. Nyborg, "The crystal structure of Cys-tRNA-Cys-EF-Tu-GDPNP reveals general and specific features in the ternary complex and in tRNA", *Structure*, Vol. 7, No. 2, pp. 143-56, 1999.

20. Yusupov, M. M., G. Z. Yusupova, A. Baucom, K. Lieberman, T. N. Earnest, J. H. Cate, H. F. Noller, "Crystal structure of the ribosome at 5.5 A resolution", *Science,* Vol. 292, No. 5518, pp. 883-896, 2001.

21. Berman, H. M., J. Westbrook, Z. Feng, G. Gilliland, T. N. Bhat, H. Weissig, I. N. Shindyalov, P. E. Bourne, "The Protein Data Bank", *Nucleic Acids Research,* Vol. 28, No. 1, pp. 235-242, 2000.

22. Schuwirth, B. S., M. A. Borovinskaya, C. W. Hau, W. Zhang, A. Vila-Sanjurjo, J. M. Holton, J. H. Cate, "Structures of the bacterial ribosome at 3.5 A resolution", *Science,* Vol. 310, No. 5749, pp. 827-834, 2005.

23. Yusupova, G., L. Jenner, B. Rees, D. Moras, M. Yusupov, "Structural basis for messenger RNA movement on the Ribosome", *Nature Letters*, Vol. 444, No. 7117, pp. 391-394, 2006.

24. Cannone J. J., S. Subramanian, M. N. Schnare, J. R. Collett, L. M. D'Souza, Y. Du, B. Feng, N. Lin, L. V. Madabusi, K. M. Müller, N. Pande, Z. Shang, N. Yu, R. R. Gutell, "The Comparative RNA Web (CRW) Site: An Online Database of Comparative Sequence and Structure Information for Ribosomal, Intron, and Other RNAs", *BMC Bioinformatics*, Vol. 3, No. 1, pp. 1-31, 2002.

25. Amit, M., R. Berisio, D. Baram, J. Harms, A. Bashan, A. Yonath, "A crevice adjoining the ribosome tunnel: hints for cotranslational folding", *FEBS Letters,* Vol. 579, No.15, 3207–3213, 2005.

26. Kagawa, Y., E., Racker, "Partial resolution of enzymes catalyzing oxidative phosphorylation", *Journal of Biological Chemistry,* Vol. 241, No. 10, pp. 2461–2466, 1966.

27. Schäfer, M., T. R. Schneider, G. M. Sheldrick, "Crystal structure of vancomycin", *Structure,* Vol. 4, No. 12, pp. 1509-1515, 1996.

28. Auerbach, T., I. Mermershtain, C. Davidovich, A. Bashan, M. Belousoff, I. Wekselman, E. Zimmerman, L. Xiong, D. Klepacki, K. Arakawa, H. Kinashi, A. S. Mankin, A. Yonath, "The structure of ribosome-lankacidin complex reveals ribosomal sites for synergistic antibiotics", *Proceedings of the National Academy of Sciences of the United States of America*, Vol. 107, No. 5, pp.1983-1988, 2010.

29. Davidovich, C., A. Bashan, T. Auerbach-Nevo, R. D. Yaggie, R. R. Gontarek, A. Yonath, "Induced-fit tightens pleuromutilins binding to ribosomes and remote interactions enable their selectivity", *Proceedings of the National Academy of Sciences of the United States of America*, Vol. 104, No. 111, pp. 4291-4296, 2007.

30. Tirion, M. M., “Large amplitude elastic motions in proteins from a single-parameter, atomic analysis”, *Physical Review Letters*, Vol. 77, No. 9, pp. 1905–1908, 1996.

31. Bahar, I., A. R. Atilgan, B. Erman, “Direct evaluation of thermal fluctuations in proteins using a single-parameter harmonic potential”, *Folding and Design*, Vol. 2, No. 3, pp. 173-18, 1997.

32. Haliloglu, .T, I. Bahar, B. Erman, “Gaussian dynamics of folded proteins”, *Physical Review Letters*, Vol. 79, No. 16, pp. 3090-3093, 1997.

33. Bahar, I., Q. Cui, *Normal mode analysis theory and applications to biological and chemical systems*, Chapman & Hall/CRC, Florida, 2006.

34. Bahar, I., L. R. Jernigan, “Vibrational dynamics of transfer RNAs: Comparison of the free and synthetase-bound forms”, *Journal of Molecular Biology*, Vol. 281, No. 5, pp. 871-884, 1998.

35. Haliloglu, T., E. Seyrek, B. Erman, “Prediction of binding sites in receptor-ligand complexes with the Gaussian Network Model”, *Physical Review Letters*, Vol. 100, No. 22, p. 228102, 2008.

36. Ozbek P., S. Soner B. Erman, T. Haliloglu, “DNABINDPROT: Fluctuation-based predictor of DNA-binding residues within a network of interacting residues”, *Nucleic Acids Research*, Vol. 38, Web Server Issue, W417-23, 2010.

37. Haliloglu, T., B. Erman, “Analysis of correlations between energy and residue fluctuations in native proteins and determination of specific sites for binding”, *Physical Review Letters*, Vol. 102, No. 8, pp. 1-4, 2009.

38. Darty, K., A. Denise, and Y., Ponty, “VARNA: Interactive drawing and editing of the RNA secondary structure”, *Bioinformatics*, Vol. 25, No. 15, pp. 1974-1975, 2009.

39. del Sol Mesa, A., F. Pazos, and A. Valencia, "Automatic methods for predicting functionally important residues", *Journal Molecular Biology*, Vol. 326, No.4, pp. 1289-1302, 2003.

40. Harms, J. M., F. Schluenzen, R. Zarivach, A. Bashan, S. Gat, I. Agmon, H. Bartels, F. Franceschi, A. Yonath, "High resolution structure of the large ribosomal subunit from a mesophilic eubacterium", *Cell*, Vol. 107, No. 5, pp. 679-688, 2001.

41. Harms, J. M., D. N. Wilson, F. Schluenzen, S. R. Connell, T. Stachelhaus, Z. Zaborowska, C. M. Spahn, P. Fucini, "Translational regulation via L11: molecular switches on the ribosome turned on and off by thiostrepton and micrococcin", *Molecular Cell*, Vol. 30, No.1, pp. 26-38, 2008.

42. Schuwirth, B. S., J. M. Day, C. W. Hau, G. R. Janssen, A. E. Dahlberg, J. H. D. Cate, A. Vila-Sanjurjo, "Structural analysis of kasugamycin inhibition of translation", *Nature Structural & Molecular Biology*, Vol. 13, No. 10, pp. 879-886, 2006.

43. Borovinskaya, M. A., S. Shoji, J. M. Holton, K. Fredrick, J. H. Cate, "A steric block in translation caused by the antibiotic spectinomycin", *ACS Chemical Biology*, Vol. 2, No. 8, pp. 545-552, 2007.

44. Borovinskaya, M. A., S. Shoji, K. Fredrick, J. H. D. Cate, "Structural basis for hygromycin B inhibition of protein biosynthesis", *RNA*, Vol. 14, No. 8, pp. 1590-1599, 2008.

45. Zhang, W., J. A. Dunkle, J. H. Cate, "Structures of the ribosome in intermediate states of ratcheting", *Science*, Vol. 325, No. 5943, pp. 1014-1017, 2009.

46. Klein, D. J., T. M. Schmeing, P. B. Moore, T. A. Steitz, "The kink-turn: a new RNA secondary structure motif", *The EMBO Journal*, Vol. 20, No. 15, pp. 4214-4221, 2001.

47. Hansen, J., P. B. Moore, T. A. Steitz, "Structures of Five Antibiotics Bound at the Peptidyl Transferase Center of the Large Subunit", *Journal of Molecular Biology*, Vol. 330, No. 5, pp. 1061-1075, 2003.

48. Tu, D., G. Blaha, P. B. Moore, T. A. Steitz, "Structures of MLSBK antibiotics bound to mutated large ribosomal subunits provide a structural explanation for resistance", *Cell*, Vol. 121, No. 2, pp. 257-270, 2005.

49. Schroeder, S. J., G. Blaha, J. Tirado-Rives, T. A. Steitz, P. B. Moore, "The structures of antibiotics bound to the E site region of the 50 S ribosomal subunit of Haloarcula marismortui: 13-deoxytedanolide and girodazole", *Journal of Molecular Biology*, Vol. 367, No. 5, pp.1471-1479, 2007.

50. Blaha, G., G. Gurel, S. J. Schroeder, P. B. Moore, T. A. Steitz, "Mutations outside the anisomycin-binding site can make ribosomes drug-resistant", *Journal of Molecular Biology*, Vol. 379, No. 3, pp. 505-519, 2008.

51. Gurel, G., G. Blaha, P. B. Moore, T. A. Steitz, "U2504 determines the species specificity of the A-site cleft antibiotics: the structures of tiamulin, homoharringtonine, and bruceantin bound to the ribosome", *Journal of Molecular Biology*, Vol. 389, No. 1, pp. 146-156, 2009.

52. Gurel, G., G. Blaha, T. A. Steitz, P. B. Moore, "Structures of triacetyloleandomycin and mycalamide A bind to the large ribosomal subunit of Haloarcula marismortui", *Antimicrobial Agents Chemotherapy*, Vol. 53, No. 12, pp. 5010-5014, 2009.

53. Carter, A. P., W. M. Clemons Jr., D. E. Brodersen, R. J. Morgan-Warren, B. T. Wimberly, V. Ramakrishnan, "Functional insights from the structure of the 30S ribosomal subunit and its interactions with antibiotics", *Nature*, Vol. 407, No. 6802, pp. 340-348, 2000.

54. Brodersen, D. E., W. M. Clemons Jr., A. P. Carter, R. J. Morgan-Warren, B. T. Wimberly, V. Ramakrishnan, "The structural basis for the action of the antibiotics tetracycline, pactamycin, and hygromycin B on the 30S ribosomal subunit", *Cell*, Vol. 103, No. 7, pp. 1143-1154, 2000.

55. Pioletti, M., F. Schlunzen, J. Harms, R. Zarivach, M. Gluhmann, H. Avila, A. Bashan, H. Bartels, T. Auerbach, C. Jacobi, T. Hartsch, A. Yonath, F. Franceschi, "Crystal structures of complexes of the small ribosomal subunit with tetracycline, edeine and IF3", *The EMBO Journal*, Vol. 20, No. 8, pp. 1829-1839, 2001.

56. Ogle, J. M., Brodersen, D. E., Clemons Jr., W. M., Tarry, M. J., Carter, A. P., Ramakrishnan, V. "Recognition of cognate transfer RNA by the 30S ribosomal subunit", *Science*, Vol. 292, No. 5518, pp. 897-902, 2001.

57. Wimberly, B. T., D. E. Brodersen, W. M. Clemons Jr., R. J. Morgan-Warren, A.P. Carter, C. Vonrhein, T. Hartsch, V. Ramakrishnan, "Structure of the 30S ribosomal subunit", *Nature*, Vol. 407, No. 6802, pp. 327-339, 2000.

58. Schluenzen, F., C. Takemoto, D. N. Wilson, T. Kaminishi, J. M. Harms, K. Hanawa-Suetsugu, W. Szaflarski, M. Kawazoe, M. Shirouzo, K. H. Nierhaus, S. Yokoyama, P. Fucini, "The antibiotic kasugamycin mimics mRNA nucleotides to destabilize tRNA binding and inhibit canonical translation initiation", *Nature Structural & Molecular Biology*, Vol. 13, No. 10, pp. 871-878, 2006.

59. Bulkley, D., C. A. Innis, G. Blaha, T. A. Steitz, "Revisiting the structures of several antibiotics bound to the bacterial ribosome", *Proceedings of the National Academy of Sciences of the United States of America*, Vol. 107, No. 40, pp. 17158-17163, 2010.

60. Seidelt, B., C. A. Innis, D. N. Wilson, M. Gartmann, J. P. Armache, E. Villa, L. G. Trabuco, T. Becker, T. Mielke, K. Schulten, T. A. Steitz, and R. Beckmann, "Structural insight into nascent polypeptide chain-mediated translational stalling", *Science*, Vol. 326, No. 5958, pp.1412–1415, 2009.

61. Polacek N., and A. S. Mankin, “The ribosomal peptidyl transferase center: structure, function, evolution, inhibition”, *Critical Reviews in Biochemistry and Molecular Biology*, Vol. 40, No. 5, pp. 285–311, 2005.

62. Yassin, A., A. S. Mankin, “Potential new antibiotic sites in the ribosome revealed by deleterious mutations in rna of the large ribosomal subunit”, *The Journal of Biological Chemistry*, Vol. 282, No. 33, pp. 24329-24342, 2007.

63. Yassin, A., K. Fredrick, A. S. Mankin, “Deleterious mutations in small subunit ribosomal RNA identify functional sites and potential targets for antibiotics”, *Proceedings of the National Academy of Sciences of the United States of America*, Vol. 102, No. 46, pp. 16620-16625, 2005.